Understanding the Forces and Energy in the Electrification System During a De-wirement

Summary report

RESEARCH AND DEVELOPMENT

Copyright

Written by:

Steven Conway, Current Collection Solutions Ltd

Nikolaos Baimpas, Atkins Global

Stephen Cullingford, Brecknell Willis

Published: December 2016

Executive summary

Section 1: Understanding the Forces and Energy in the Electrification System During a De-wirement

Industry stakeholders have expressed the need for an improved understanding of the forces and energy in electrification systems during de-wirements, reviewing both sides of the vehicle/infrastructure interface.

The problem that this research sets out to address is that with the increasing use of polymeric and composite insulators on both overhead line equipment (OLE) and the insulators supporting the pantograph base, there is insufficient understanding of the transfer of forces and energy through the system components to enable the failure modes to be optimised.

Littleport incident review

The review concludes that it is evident that the pantograph did not fail as described in the RAIB report but there in insufficient documented evidence or photographs to come up with a more plausible scenario.

Understanding the Forces and Energy in the Electrification System During a De-Wirement

Calculations were carried out to ascertain the forces required to:

- Fracture four ceramic pantograph foot insulators
- Distort the OLE mast
- Consider using the forces calculated to design a frangible link(s) in the pantograph articulation

As a result of calculations, the report concluded:

- Ceramic pantograph foot insulator = 18.4kN maximum fracture load in shear
- Ceramic cantilever insulator = 7.45kN maximum fracture load in shear
- Polymeric pantograph foot insulator = 900 MPa maximum capacity of polymeric core in shear
- Polymeric cantilever insulator = 217MPa minimum load capacity in shear
- Permanent deformation of OLE structure = 43kN in along-track force applied on single-track cantilever
- Three and four-foot pantograph with polymeric insulators = 352kN due to tensile failure of the top pantograph arm
- Four-foot pantograph with ceramic insulators = 70kN due to shear failure of pantograph foot insulators

Section 2:
Controlling the failure modes of the pantograph and OLE structure during a de-wirement

The report details methods on the pantograph and OLE for controlling the failure modes and recommended the following should be considered:

- Precise information for individual material deformation parameters via mechanical testing will allow the optimisation of the fail-safe design implementation into pantograph and OLE system.
- Experimental investigation on proposed fail safe system components at material level.
- Experimental dynamic assessment on proposed fail-safe system components full scale assembly in a controlled environment.

Once the final design and prototype fail safe devices are installed these should be tested individually to ensure that they behave as per FE mechanical simulation.

Understanding the Forces and Energy in the Electrification System During a De-wirement

Section 1: Understanding the forces and energy in the electrification system during a de-wirement

1 Introduction

Industry stakeholders have expressed the need for an improved understanding of the forces and energy in electrification systems during de-wirements, reviewing both sides of the vehicle/infrastructure interface.

There have been significant de-wirement incidents over the past 15 years resulting in risk to passengers, damage to infrastructure and rolling stock and considerable delays and costs to the GB rail network.

On 5 January 2012, one such de-wirement incident occurred at Littleport, Cambridgeshire. Due to several causal factors, an impact broke several ceramic pantograph insulators on which the pantograph assembly was mounted, allowing it to fall from the roof, breaking two body-side windows and resulting in three minor injuries to passengers inside the train, in addition to extensive damage to overhead line equipment. The subsequent RAIB (Rail Accident Investigation Branch) accident report issued a learning point that "consideration should be given to using polymeric or composite insulators to support train pantographs, as they have the potential to mitigate the risks arising from pantographs hitting structures." However, the report also stated that "polymeric and composite insulators are more likely to distort and absorb energy during an impact than ceramic insulators".

The way in which components fail during a de-wirement can limit or exacerbate the damage to rolling stock and infrastructure, and also have safety implications. Ceramic insulators tended to be the known location of failure (frangible) during a de-wirement, however with increasing numbers being replaced by a much stronger polymeric/ composite insulator, the frangibility joint has moved elsewhere within the system. This has led stakeholders to express concerns that the use of these insulators had the potential to indirectly cause further damage to OLE, with potential to lead to train derailments if damage leads to debris on the line. The problem that this

research sets out to address is that with the increasing use of polymeric and composite insulators on both OLE and the insulators supporting the pantograph base, there is insufficient understanding of the transfer of forces and energy through the system components to enable the failure modes to be optimised.

Figure 1 - Main pantograph components

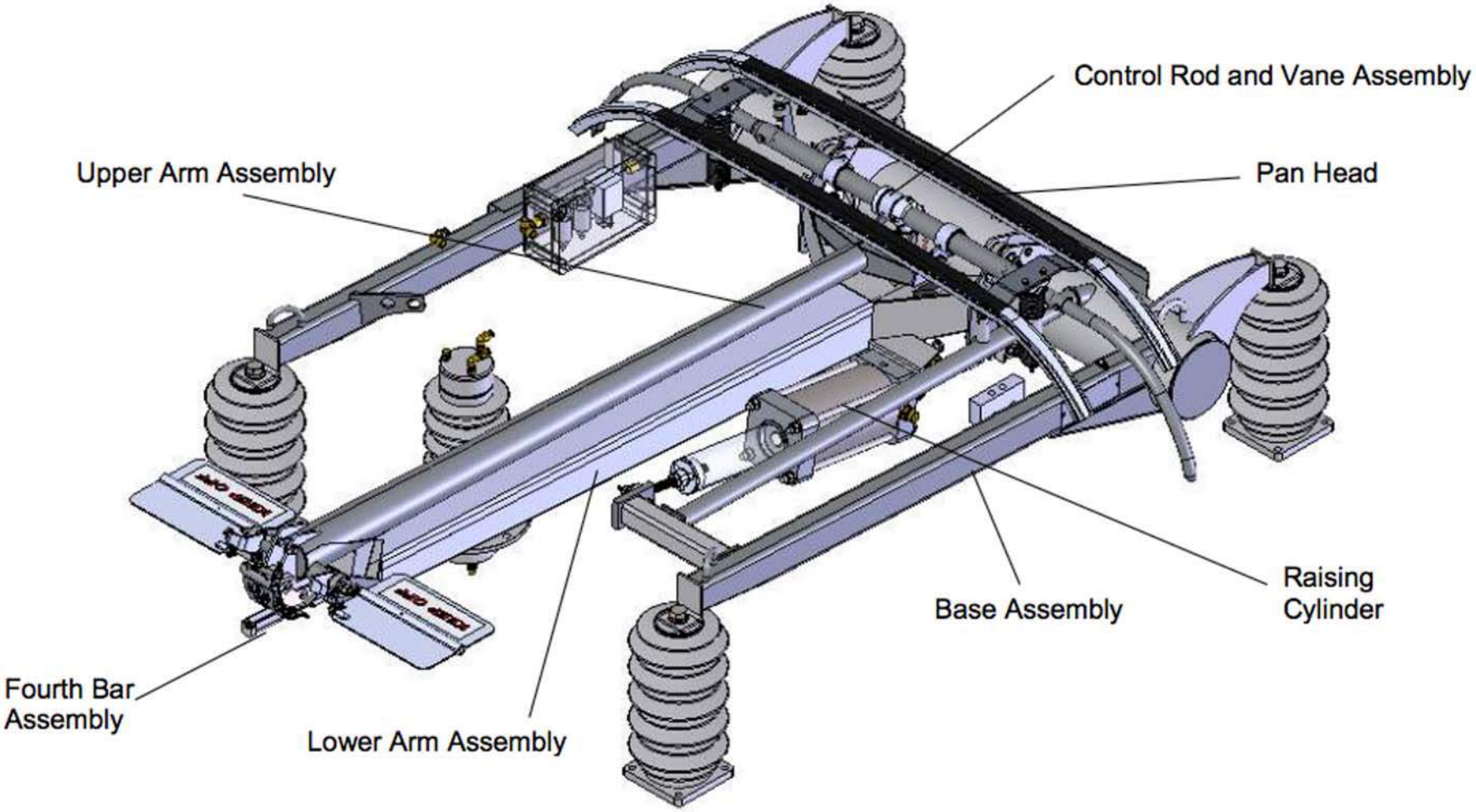

2 Findings from previous report on the desktop review of incident reports

The initial research comprised an in-depth review and analysis of all incident reports provided by Network Rail dating from 2005. Unfortunately, after 2011 only two reports had sufficient detail to carry out any meaningful analysis.

The analysis identified seven trends:

1 Fractured pantograph horns
2 Pantograph pulled backwards with upper and lower arms close to horizontal
3 Pantograph pulled off the vehicle roof
4 Pantograph with knuckle uppermost
5 Pantograph chain failure
6 Failure of Arthur Flury Neutral section
7 14 of the 34 incidents analysed occurred within 1km of a station, underbridge or level crossing

The analysis also identified there were three incidents of concern, any of which could have caused serious injury to staff or the public. These incidents included reports where pantographs had been pulled of the roof of vehicles and an OLE mast distorted.

The following recommendations were made:

1 Calculate the forces required to:
   a Fracture four ceramic pantograph foot insulators
   b Distort the OLE mast
2 Consider using the forces calculated to design a frangible link(s) in the pantograph articulation
3 To limit the risk to staff or the public consider the secondary retention of any detached items that occur as a result of the above (2)

The knowledge obtained by calculating the above could be used to limit the damage to the rolling stock and infrastructure by designing frangible joints on the pantograph.

3 Littleport review

The RAIB report 06/2013 v2 'Accident involving a pantograph and the overhead line near Littleport, Cambridgeshire 5 January 2012, page 23 paragraph 72 states that:

> *'As a result of the impact at mast C118/32, the pantograph arm buckled, the constraint chains in the pantograph joints broke, and the pantograph started to collapse, all as designed. In addition, the four ceramic post insulators on which the pantograph frame was mounted broke, meaning that the pantograph assembly was no longer secure on the train roof. However the pantograph assembly remained in position in the pantograph well (paragraph 39).'*

Under normal operating circumstances the centre chain would fail at a relatively low force (it is not designed as a frangible link as inferred in the report) and would not transfer the forces to the base frame and insulators. Something else had to occur to transfer such high loads as to shear the insulators, such as engagement by the lower arm with trackside structure.

There are no photographs of pantograph damage in the report to prove or disprove the reported theory.

Approximate calculations have been carried out and in order to cause the top arm of the pantograph to buckle (the presumption is that it is the top arm as there are no photographs) will require 375kN. This is at least 5 times more than the 4x18kN cantilever load that is required to break the four pan base insulators.

This means that the pantograph arm was either bent due to vertical loads applied whilst the pantograph was trying to unfold (normal operation geometry) as a result of interacting with the OLE infrastructure. Or it occurred as a result of impacting to a structure after unfolding as we have seen in several images from other reports.

In summary there is insufficient evidence to sustain the buckling of the pantograph neither does it seem like a feasible scenario. Therefore, unless the pantograph was fully unfolded and entangled with the OLE infrastructure it seems impossible to be able to deliver the required force for the insulators to fail.

It is not doubted that the root cause of the incident was the movement of the structure exacerbated by high winds; what is questioned is the failure scenario of the pantograph and insulators.

There is insufficient evidence documented in the report to come up with a more credible failure scenario.

4 Simulation input information

The list of input drawings below has been provided by Brecknell Wills, Network Rail and ATKINS to facilitate the modelling process. Details and drawings are given in Appendix A.

- Ceramic 14'' Pantograph Foot Insulator
- Polymeric 14'' Pantograph Foot insulator
- Ceramic cantilever insulator
- Polymeric cantilever insulator
- 3-Foot Thameslink Pantograph GA – M00042-54-L
- 4-Foot GA CL91 Pantograph – M00042-10-L
- Mark 3B STC OLE Cantilever – 254 x 254 x 73 OLE mast installation

The schematic representation of the 3D solid model for the ceramic foot insulator is shown in Figure 2. Different materials such as cement and cast iron are highlighted in different colours (Figure 2(a)). Meshing of individual insulator components is shown in the final assembly in Figure 2(b). An example of a typical STC structure in a 3D model using Euler beam elements for construction is given in Figure 3. The example was chosen as it is common for these structure to suffer from inelastic deformation during de-wirement incidents. The structure is a Mark 3B STC OLE Cantilever with a 254 x 254 x 73 OLE mast.

Representations of the pantograph assemblies are shown in Figure 4. The 3-foot pantograph will be introduced in increasing numbers alongside the 4-foot. Respective mass models were used for the spring rates of the pantographs.

Figure 2 - (a) 3D solid model Rendering of Ceramic pantograph foot insulator (b) 3D meshing of the assembly.

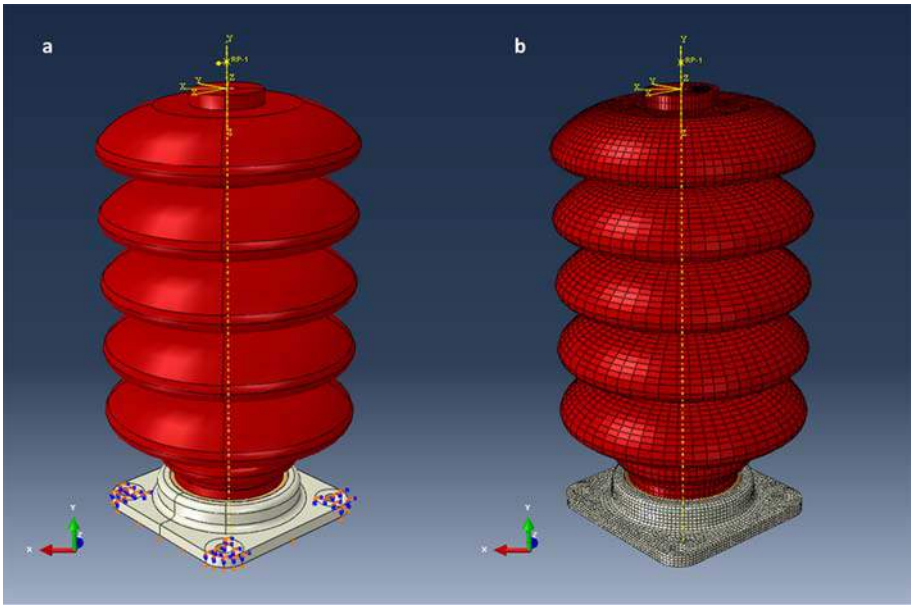

Figure 3 - 3D Euler beam model for a typical Mark 3B STC OLE structure.

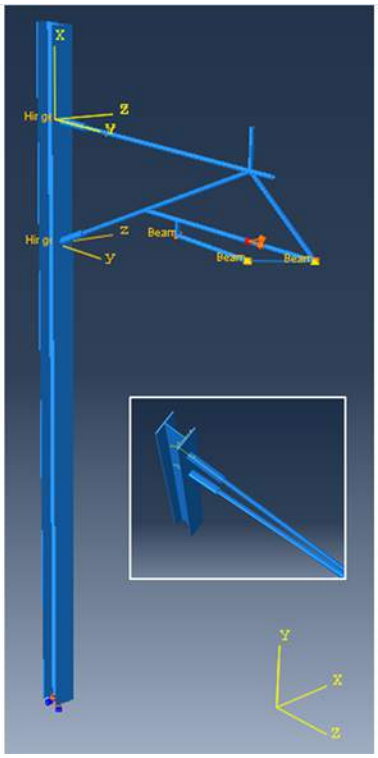

Figure 4 - 3D Euler beam model for a typical (a) 3-Foot Pantograph; and (b) 4-Foot Pantograph.

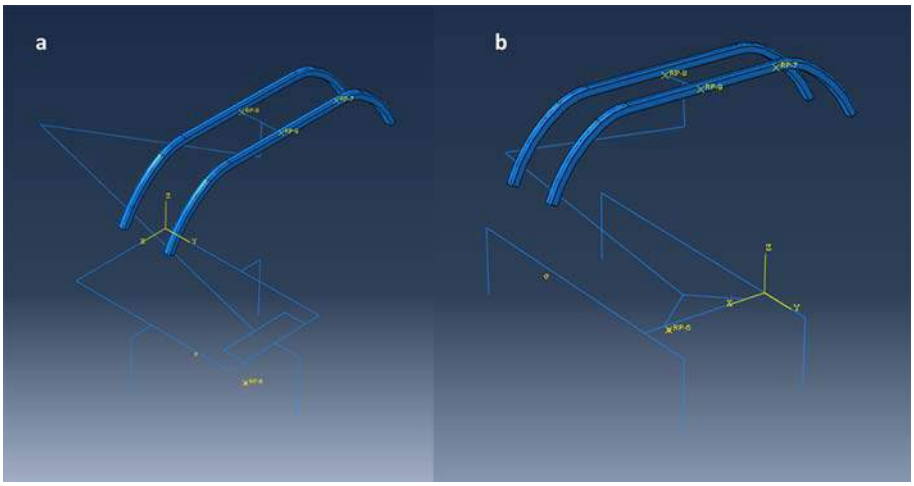

Note: The pantograph heads have been used as solids.

Materials testing reports (Details are given in Appendix A.):

- Uniaxial testing of 14'' Polymeric Pantograph Foot insulator (max. 100kN)
- Uniaxial testing of 14'' Ceramic Pantograph Foot insulator (max. 100kN)
- Cantilever load application on 14'' Polymeric Pantograph Foot insulator (max. 15kN)
- Cantilever load application on 14'' Ceramic Pantograph Foot insulator (max. 15kN)

5 Insulator component results

The first part of the investigation aims to describe the mechanical deformation behaviour of polymeric and ceramic insulators. Historically, porcelain ceramic insulators have been used for high voltage applications as an effective way to electrically isolate structures and wire components. Porcelain insulators have a content of >99 % of Al2O3 aluminium oxide, as a result of high-temperature furnace process with final surface glazing. The final coating ensures weather protection and improves resistance against surface defects, such as cracks that can significantly lower the mechanical strength of the insulator.

The result of the manufacturing process is a brittle component insulator which behaves better in compression and is more vulnerable to tensile and bending load application. Even though the core material behaviour is uniform the high temperature processing results in the formation of voids (trapped air inclusions) within the component bulk whose size and distribution are difficult to determine by macroscopic examination. In case of a tensile load being applied the voids will act as a local stress concentration spot that will enable the formation of cracks. Upon crack initiation the brittle nature of the material will result in quick crack propagation, hence fracturing and component failure.

A more modern solution has been introduced with the use of epoxy resin insulators reinforced with uniaxial glass fibres. This solution has significant advantages as the polymeric insulators are lighter and easier to install, require low maintenance, have longer in-service life span and are stronger and more resistant to breakage. The increase of load capacity and the inherent ability of polymers to sustain large deformations without breaking has severe repercussions in the case of accidental pantograph de-wirement incidents. The polymeric insulators are not susceptible to failure under cantilever loads and high strain rates experienced during impact as oppose to the previous generation of ceramic insulators. As a result the damage caused in the network is more significant and consequently concerns have been raised for the safety of passengers and working personnel.

5.1 Materials calibration

This section describes the steps followed to determine the individual material properties. The different insulators consist of different parts and made out of different materials. Accurate determination of material properties (elastic and ultimate) together with the characteristic component geometry allows for precise determination of mechanical response under various loading conditions. Additionally, assumptions had to be made for non-existing material specific information such as non-uniform modulus of elasticity for the polymeric insulator or void content for the ceramic insulators.

5.1.1 Ceramic insulators

Ceramic insulators consist of a ceramic component, containing the characteristic sheds and a cast iron base(s) (Figure 2). Portland cement is used for adhesion between the two parts. Literature material specifications were used for Portland cement and cast iron insulator ends. A starting generic value for Young's modulus was given to the ceramic component. The resulting deformation under cantilever and tension load was then compared and adjusted to the experimental data from Brecknell Willis testing results for uniaxial tension up to 100kN and cantilever load application up to 14kN.

Figure 5 shows the overlap between the FE simulation data and experimental data. Results represent the same set of material properties being used for both the experiments and show a remarkable difference in terms of the resultant modulus of elasticity (stiffness) for the porcelain.

Figure 5 - Ceramic 14" pantograph foot insulator experimental results compared against FE model results from cantilever and uniaxial tensile testing.

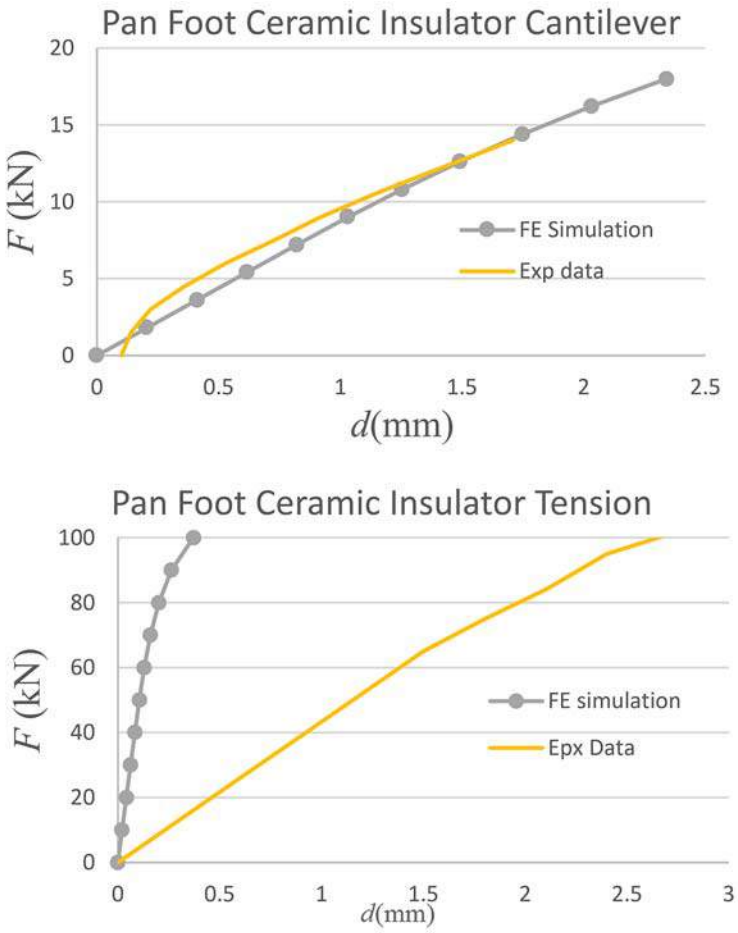

The material properties that were determined as a result of the material calibration process for cement, porcelain and cast iron are given in Table 1. The cantilever test results are closely matched with the Finite Element Model (FEM) results using a 55GPa elastic modulus from literature. The tension experiment would suggest that a <10GPa elastic modulus would be used for the porcelain. This value is well out with the margins expected in the case of a brittle ceramic material. Therefore, the properties shown in Table 1 have been used throughout the FE modelling procedures.

Table 1 - Ceramic insulator calibrated mechanical properties used for FE analysis

Cast iron	
Elastic Young's modulus	110GPa
Poisson's ratio	0.3
Plastic	
Yield stress	Plastic strain
107.51	0
119	0.016
130.55	0.032
142.08	0.054
152	0.071
162.3	0.101
172.5	0.136
Cement	
Elastic Young's modulus	31 GPa
Poisson's ration	0.215
Porcelain	
Elastic Young's modulus	55 GPa
Poisson's ration	0.16

5.1.1.1 Pantograph foot insulators (ceramic)

Additional type testing (BW15523) results for ceramic insulators were used to determine the load threshold for failure under cantilever load application. The report summarises that ceramic insulators will fail at approximately 18.4kN by porcelain fracture or as a result of the porcelain part being pulled out of the containing flange. A 3D Finite element model was developed and 18kN cantilever load was applied to match the experimental layout. The bottom flange is constrained at the bolt head locations and the underside to realistically represent the experimental boundary conditions.

Figure 6 - Ceramic Pantograph foot insulator results for cantilever load up to 18kN

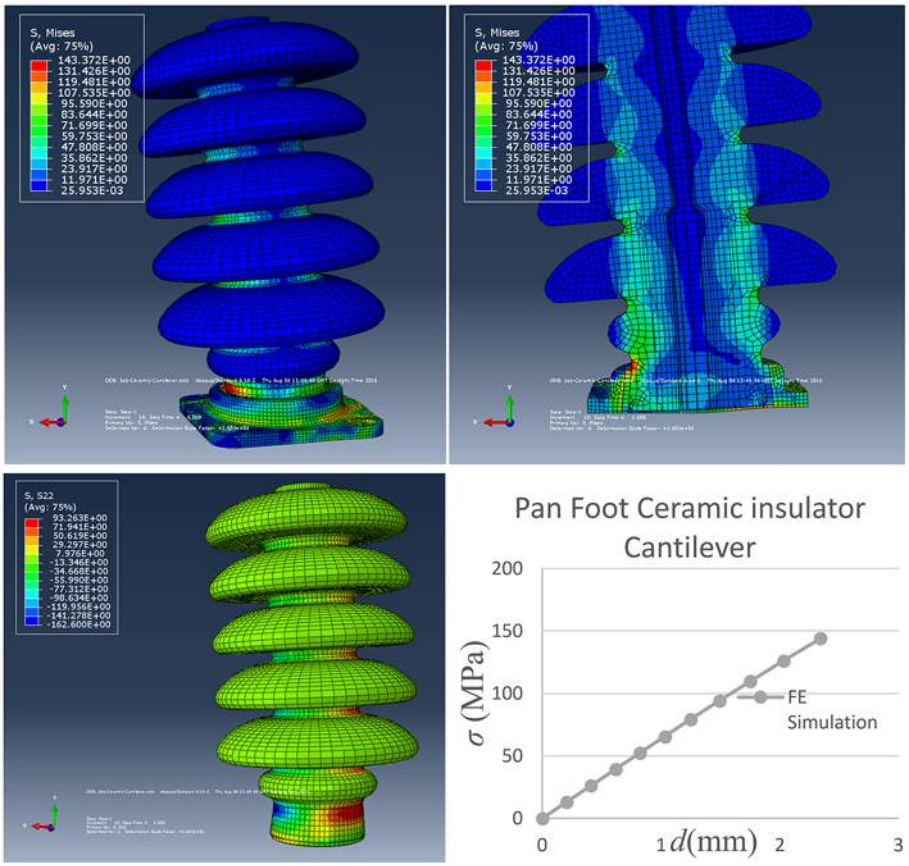

Figure 6 shows the contour 3D rendering of the Von Mises criterion showing maximum load concentration at the bottom of the insulator at the interface with the cast iron base. A cross-section is presented to show the exact location of maximum compression. Compressive and tensile stresses are separately illustrated as they are the main components that will indicate the porcelain material mechanical limits. Maximum tension (S22) is 93MPa as oppose to 162MPa in compression. As the insulator is more likely to fail in tension (due to crack propagation) 93MPa can be considered to be a realistic limit for ceramic foot insulator strength.

The ceramic foot insulator model is then subjected to a 100kN tensile load as per experiment. Due to the large diameter of the ceramic component at this load the local stress in axis component does not exceed 55MPa (see Figure 7). The ceramic insulator is not expected to fail for applied tension of 100kN,

which was confirmed by the Brecknell Willis experimental results. A likewise 3D stress contour representation is given in Figure 7 for Von Mises and S22 stress direction. Significant stresses are located in the cast iron baseplate which will cause some limited permanent deformation. The cement adhesive is not likely to sustain damage, as by default will be in compression. Even if cracks are developed at loads higher than 30MPa due to the tight fit between the porcelain insert and the cast iron base, there is no indication of separation between them. The ultimate strength of the pantograph foot insulator in tension cannot be determined with the information available. During the experiment the sample was not tested to destruction and there is little information to relate to the material composition and defects due to the manufacturing process.

Figure 7 - Ceramic Pantograph foot insulator results for tensile load up to 100kN

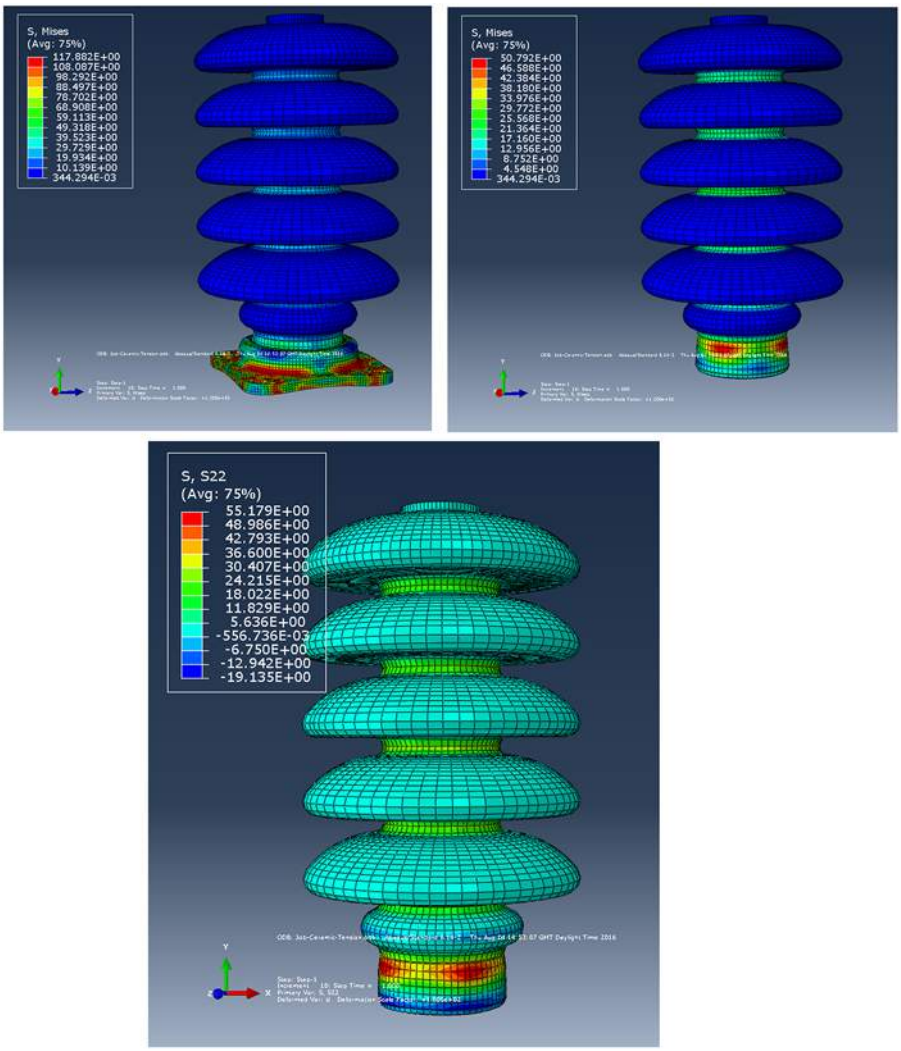

5.1.1.2 OLE cantilever insulator (ceramic)

A 3D Finite element model was developed for the OLE cantilever insulator and 18kN cantilever load was applied. As per drawing (see Appendix A) top and bottom flanges have been modelled with the exclusion of the top and bottom clamp arrangement. Similar results are obtained as shown in Figure 8 with the stresses being slightly higher compared to the pantograph foot insulator due to the longer layout and the geometry of the bottom of the insulator and the base. Comparison between the OLE cantilever and pantograph foot insulator is given in Figure 10 for stress vs displacement. It has to be highlighted that OLE cantilever insulators are not likely to be subjected to bending as they are

attached to the mast via hinged connections to avoid transmitting torsion to the slender OLE structure masts.

Figure 8 - Ceramic cantilever insulator results for cantilever load up to 18kN.

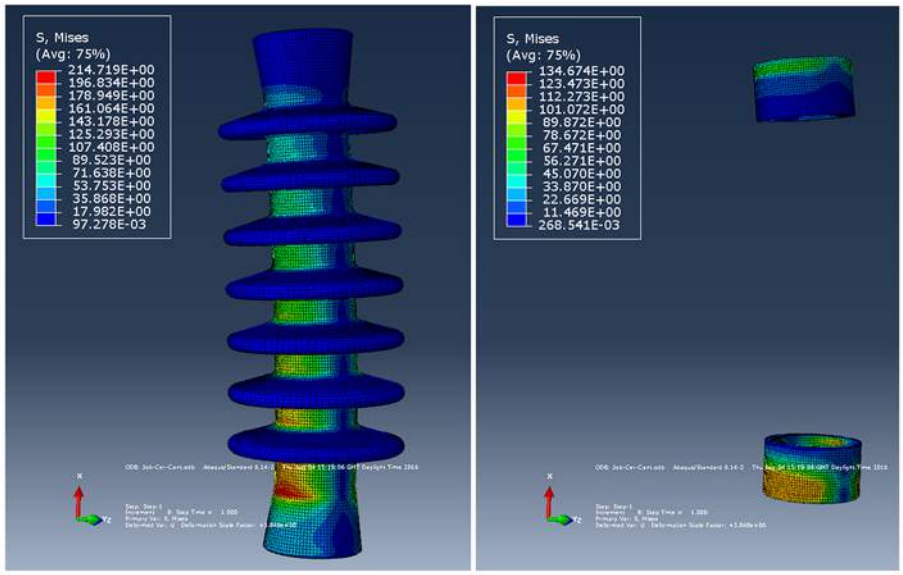

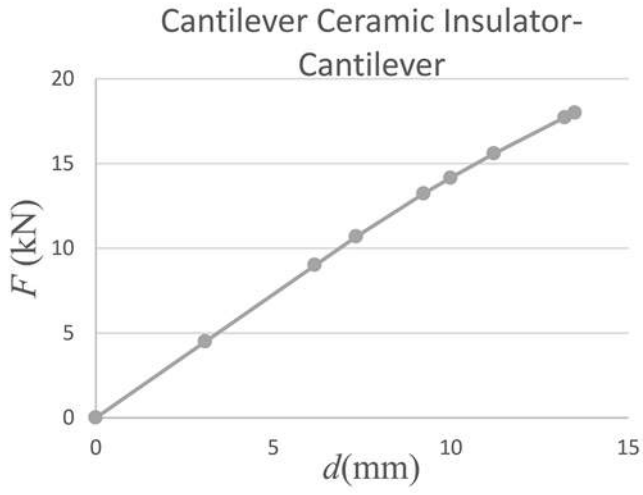

The OLE cantilever insulator model is then subjected to a 100kN tensile load. Due to the large diameter of the ceramic component at this load the local stress in axis component does not exceed 36MPa (see Figure 9). The ceramic insulator is not expected to fail for applied tension of 100kN which was confirmed by the Brecknell Willis experimental results. Significant stresses are

located in the cast iron baseplate which will cause some limited permanent deformation. The stresses in the bulk porcelain part remain low and are not likely to cause a component failure for that loading.

Figure 9 - Ceramic cantilever insulator results for tensile load up to 100kN.

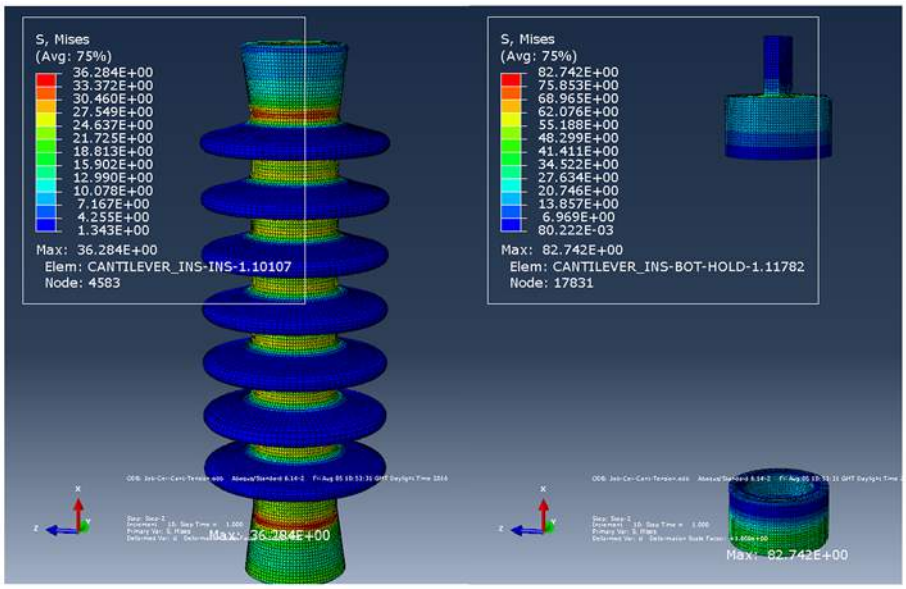

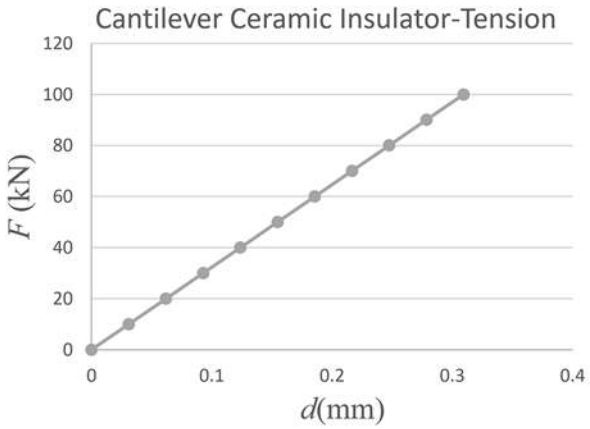

Figure 10 - Ceramic cantilever Vs pantograph foot insulator results for stress (element of maximum compression) vs deflection.

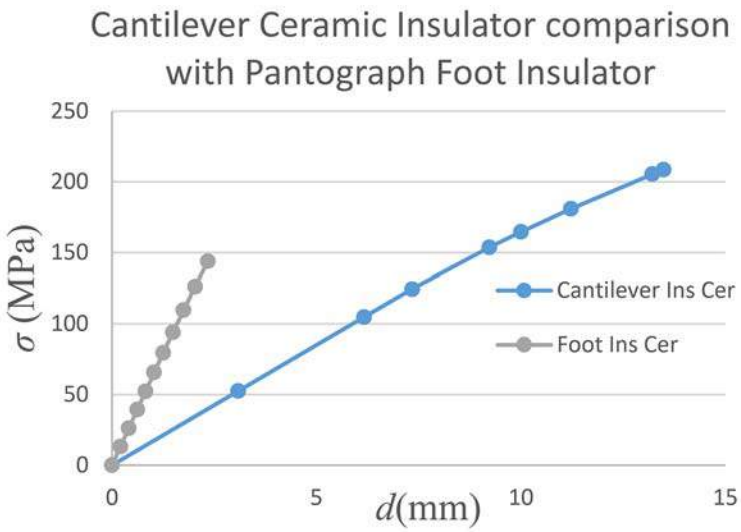

5.1.2 5.1.2 Polymeric insulators

Polymeric insulators are currently the mainstay in the industry bringing significant improvements during installation and maintenance. They are also more resistant to accidental breaking and manifest remarkable mechanical strength. The core material is made up of axially aligned microscopic glass fibres impregnated in epoxy resin. The output product is in the shape of a cylinder that is then cut into appropriate sections and crimped into aluminium end fittings to allow for mounting into the system. Elastic weather sheds are added for increased electrical insulation. Those sheds are considered not to have considerable mechanical resistance to deformation and were not taken into consideration in the analysis.

Figure 11 - Polymeric 14" pantograph foot insulator experimental results compared again FE model results from cantilever and uniaxial tensile testing.

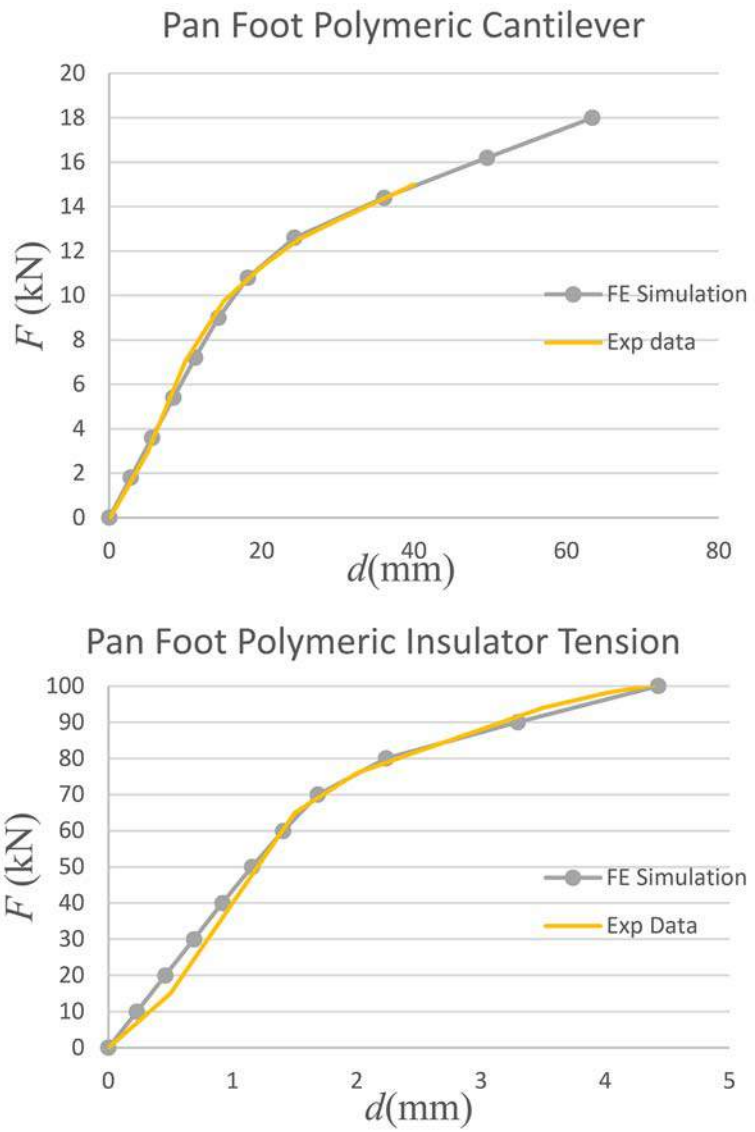

The axial distribution of glass fibres significantly enhances the strength of the polymer in tension but at the same time results into a non-uniform response to cantilever loading. Due to missing material properties required for the population of the 3D modulus of elasticity matrix, the polymeric insulators were modelled with a uniform material and with separate values for the

modulus of Elasticity for tension and Cantilever bending. Separate values for the plasticity where calculated to match the experimental results available and are given in Table 2. Results for the correlation between experimental and FE modelling are shown in Figure 11.

Table 2 - Polymeric insulator calibrated mechanical properties used for FE analysis.

Table 3 -

Polymeric foot insulators			
Cantilever (bending)		Uniaxial tension	
E (GPa)	v	E (GPa)	v
4279	0.1	1905	0.1
Plasticity properties		Plasticity properties	
Stess (MPa)	Strain	Stess (MPa)	Strain
70	0	21	0
77	0.042	24	0.003
115	0.057	40	0.0425
230	0.09	80	0.15
400	0.12		
Polymeric cantilever insulators			
E (GPa)		v	
4279		0.1	
Plasticity properties			
Stess (MPa)		Strain	
90		0	
230		0.015	
400		0.025	

5.1.2.1 Pantograph foot insulator (polymeric)

A pantograph polymeric insulator was subjected to an 18kN cantilever load and results are presented in Figure 12. FE simulation for tension was also performed up to 100kN to get comparable results with the ceramic counterparts. Results for the tension experiment are shown in Figure 13.

Figure 12 - Polymeric pantograph foot insulator results for cantilever load up to 18kN

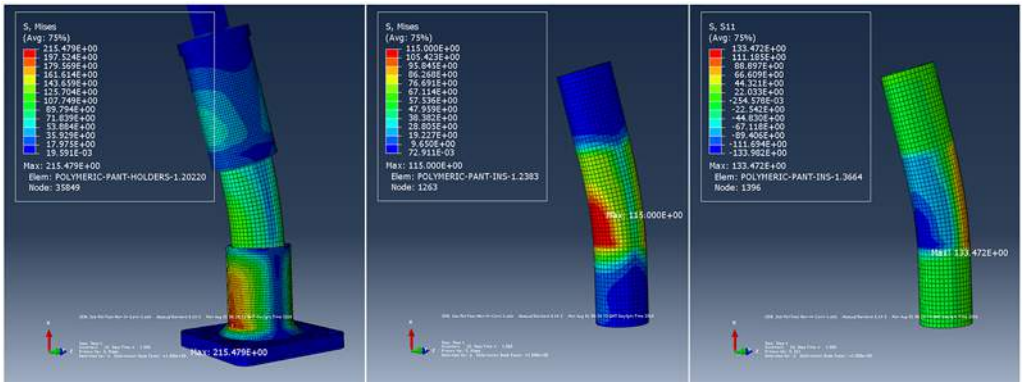

Figure 13 - Polymeric pantograph foot insulator results for tensile load up to 100kN

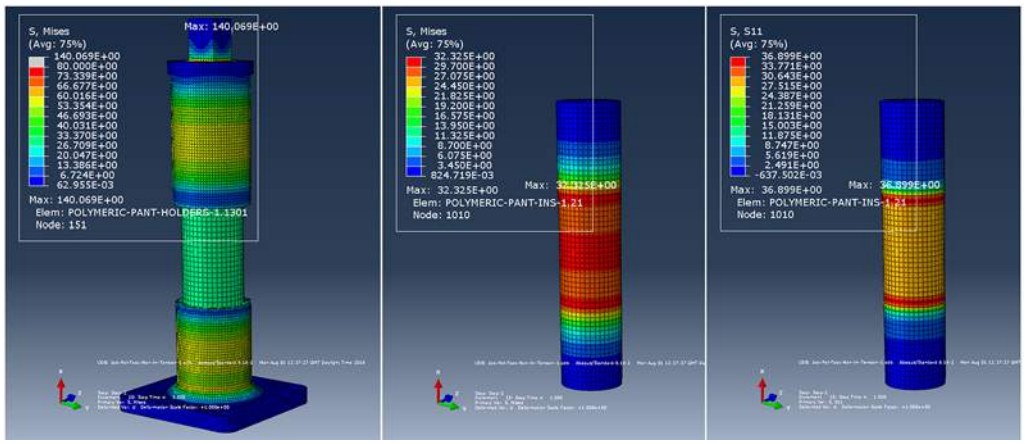

5.1.2.2 OLE cantilever insulator (polymeric)

The material properties were calibrated to match the bending deformation information of the drawing supplied by Network Rail. The modulus of elasticity was calibrated to 25GPa and deformation was correlated by applying 1000Nm, which was considered to be in the elastic zone and 3000kN (Fcant=5.6kN) in the plastic region. The calibrated modulus of elasticity shows good correlation with data supplied by a literature review. The overall deformation of 10mm at 1000Nm and 15mm at 3000Nm have been calibrated with plasticity (stress-strain) parameters being implemented into the model. The results are shown in Figure 14.

Figure 14 - Polymeric cantilever insulator results for cantilever load up to 5.6kN. Maximum deflection 69mm. Modulus of Elasticity 25kN.

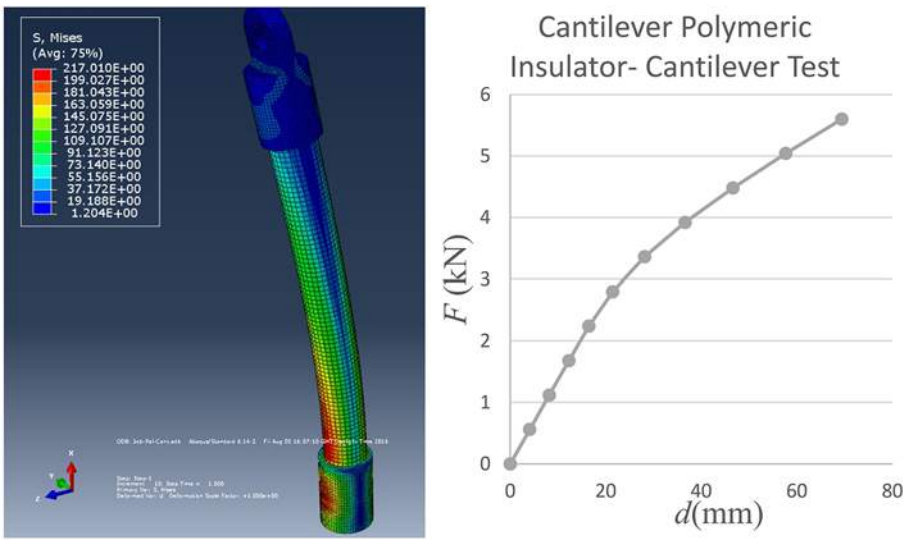

Note: Calibration of material properties has been carried out according to specification drawing supplied by NR.

Similarly, a tensile FE simulation was carried out to a maximum 90kN of uniaxial force applied to reveal the critical stress required to cause the insulator to fail. The stresses are shown in Figure 15 do not exceed 70MPa for the polymeric core.

Figure 15 - Polymeric cantilever insulator results for tensile load up to 90kN.

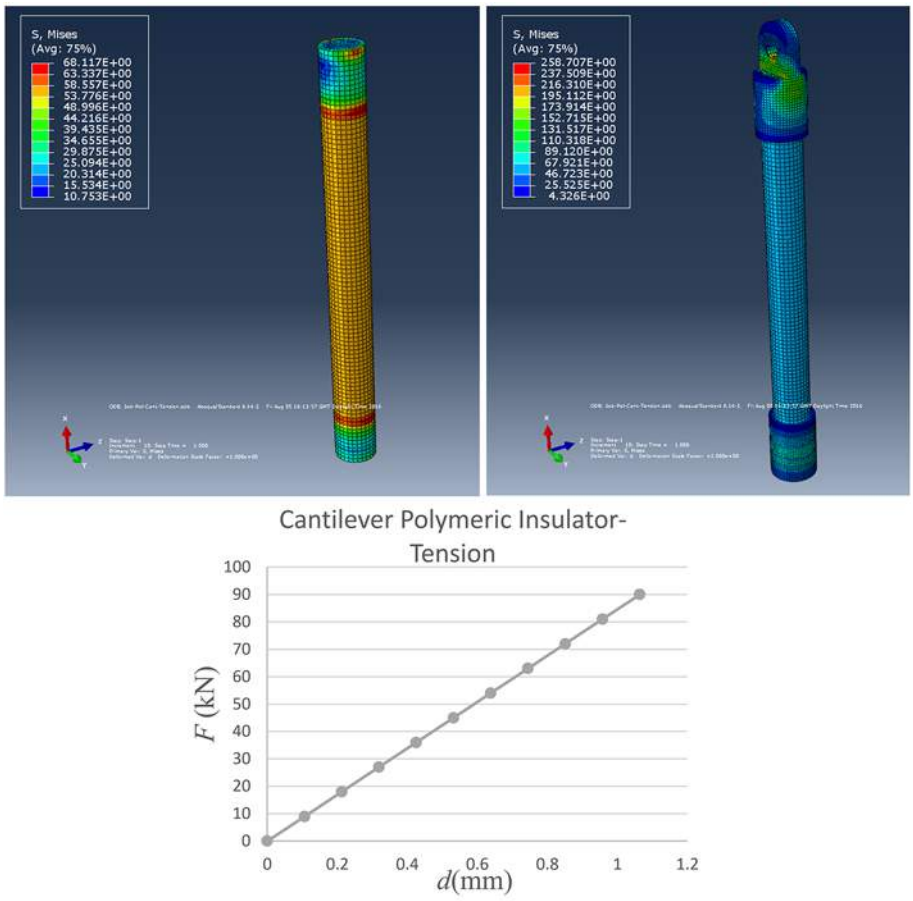

Figure 16 - Stress (at maximum compression element) Vs Applied cantilever load for cantilever and pantograph foot insulators.

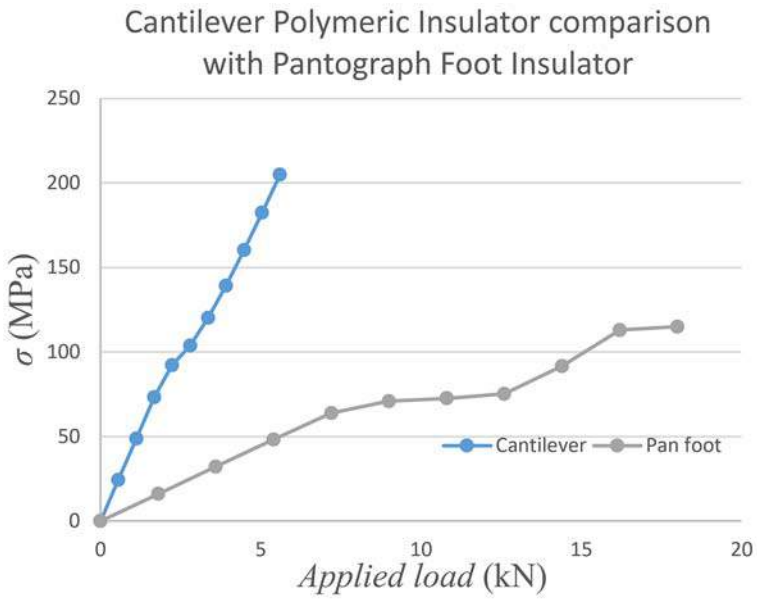

6 De-wirement simulation: Pantograph to OLE system interaction

Pantograph de-wirement incidents result in extremely complex high velocity physical and mechanical interactions between the pantograph, OLE wires and structures. Preliminary simulation and scrutinizing of the on-site de-wirement incident reports reveals that the OLE droppers will potentially be the first obstacle to the pantograph which will not be able to withstand the impact forces due to the accelerated mass of the pantograph strip and upper arm. As a result, the extended pantograph will, in most cases, impact the OLE structure and increase the risk of heavier components sustaining damage.

Additionally, the direction of travel plays an important role into the 'unfolding' geometry of the pantograph. When the pantograph is travelling knuckle leading, as shown in Figure 17, the lower arm will eventually reach the rotation limit of the uplifting hydraulic cylinder and stop. This is considered to be the most severe situation when the lower arm is extended approximately 2m above the train roof and is strongly attached through the rigid pantograph base and 3-4 polymeric foot insulators.

Figure 17 - Simulation of the pantograph travelling knuckle leading.

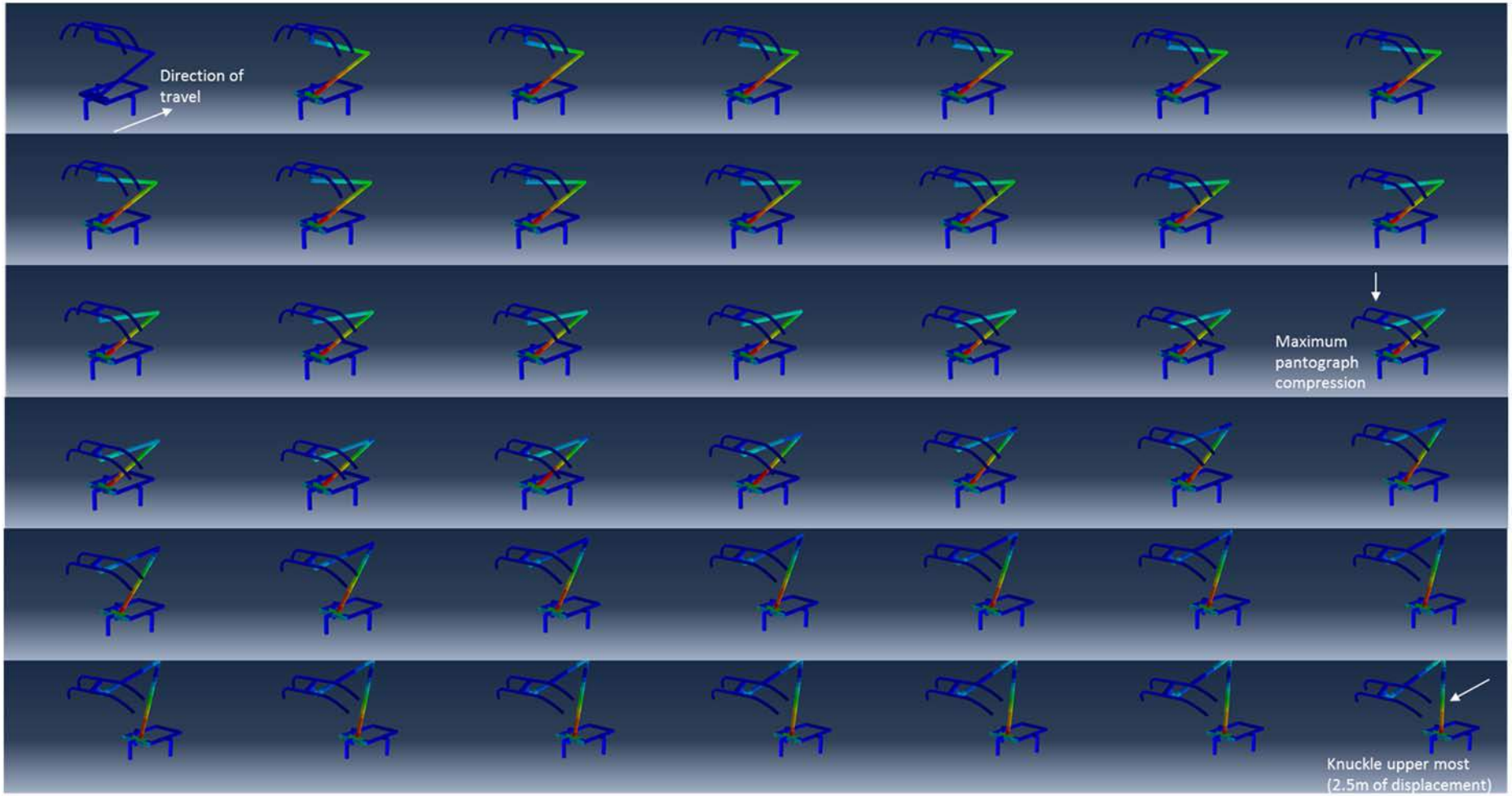

Note: The pantograph strip is restrained along and across track moving. Vertical movement and rotations are allowed. As a result of contact with the OLE cantilever the pantograph is compressed and lowered. After reaching a critical compression where the knuckle chain will fail the lower arm starts to rotate away from the pantograph base. The lower pantograph arm will stop as soon as it reached an angle where the maximum limit of compression for the pneumatic raising cylinder is reached.

Figure 18 - Simulation of the pantograph travelling knuckle trailing

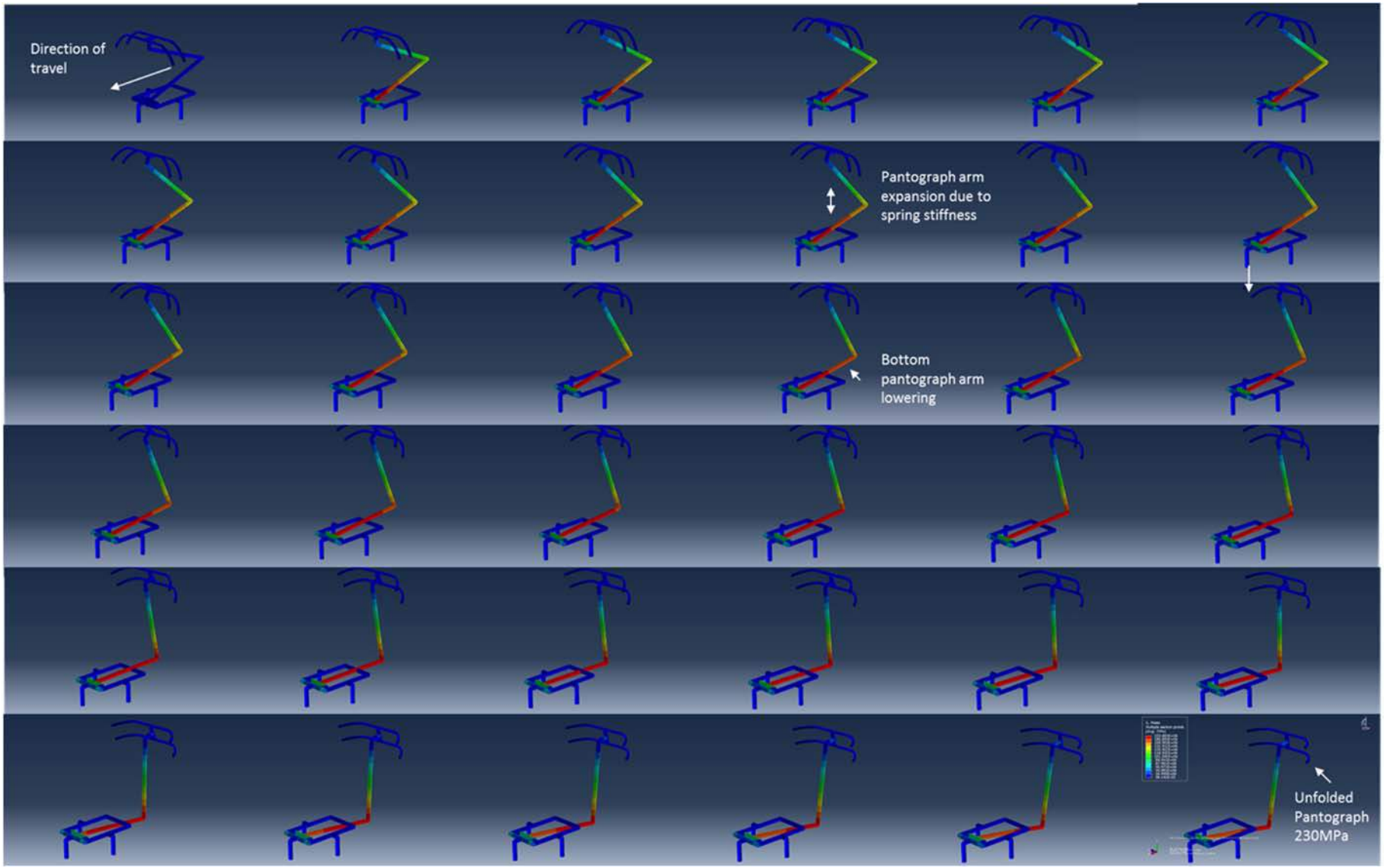

Note: The pantograph strip is restrained along and across track moving. Vertical movement and rotations are allowed. As a result of contact with the OLE cantilever the pantograph is extended and raised. After reaching a critical position of expansion the lower arm will start retracting towards the pantograph base. At the final point the pantograph lower arm is fully retracted the top arm is unfolded and the hinge connection between them is unrestrained due to breakage of the chains.

When travelling knuckle trailing as shown in Figure 18 the pantograph upon contact with the OLE will start expanding. At the last stage the pantograph will completely unfold and the force will be transmitted through the pantograph strip to the base. This situation is considered to be less destructive for the system as the pantograph upper arm and pantograph strip are lighter and have less loading capacity. Those components can be detached from the rest of the pantograph in a controlled manned and less likely to cause extensive failure to other parts of the infrastructure.

With the system complexity in mind the pantograph and the OLE mast were separately examined in a FE environment. The applied forces in the interface between the pantograph and the OLE mast were cross-correlated in order to determine the order at which different parts of the system will start failing. This focused on:

1 The required force to permanently deform an OLE mast.

2 The forces required to cause the pantograph insulators to fail.

It has to be emphasised that at this stage a static approximation for solving the FE models was agreed to be used due to the numerous components, large geometrical transitions and deformation. The accelerated mass of the pantograph will significantly impact on the applied forces to the OLE system and the individual material strain rate responses will influence their ability to absorb the impact energy. By assuming that the materials such as steel are not strain rate dependant the maximum applied force results might not be precise, nevertheless the force distribution through the system components can be accurate. Despite decreasing the confidence of maximum force values, the static approximation allows for a less onerous FE modelling exercise to be performed.

6.1 OLE Single track cantilever large scale deformation and stress distribution

Figure 19 - Schematic of the OLE mast loading via specifying along track displacement due to the pantograph impact and across track to represent the resistance of the pre-tensioned contact wire (CW) and catenary wires.

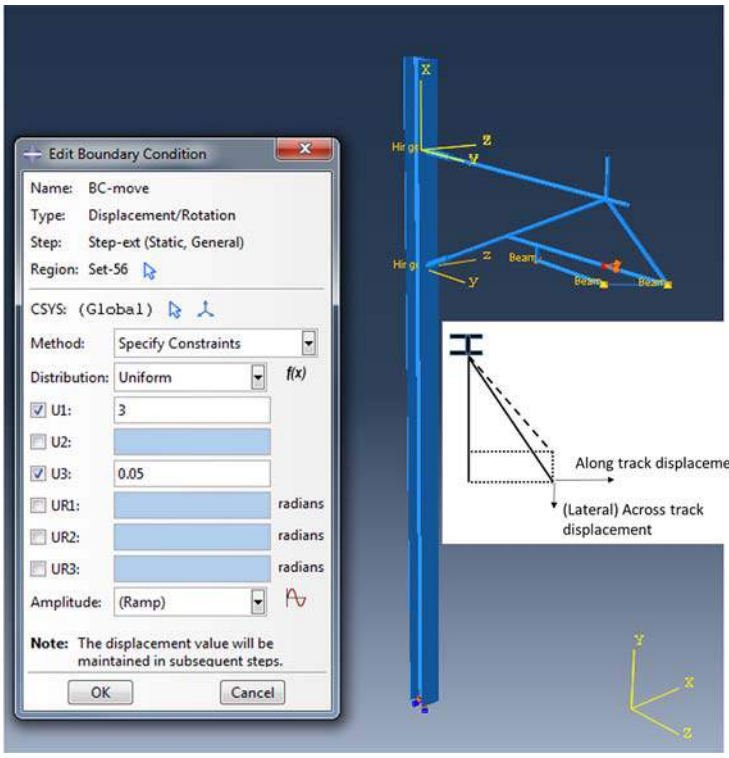

Note: The cantilever is attached to the mast via a hinged connection, which does not allow for torsional loads to be passed on to the mast. The position for load application has been chosen as it is in close proximity to the registration arm and allows for significant loads to be transmitted through to the mast. The registration arm connection is not capable of withstanding the forces of the passing pantograph. The overall displacement is as a result of the pantograph pulling along track (3m displacement) and the Catenary and CW pulling across track (0.2m displacement) due to pretension in the system. By assigning along track displacement the STC will swing around the hinged connection (see dashed line in the plan view schematic). The additional lateral displacement (0.05m) compensates for the suspended wire resistance to the rotation and keeping a constant straight pantograph pulling direction.

Figure 20 - (a) Shows the mast deformed shape and the position where force is applied. (b) Gives the overlay of undeformed and deformed states.

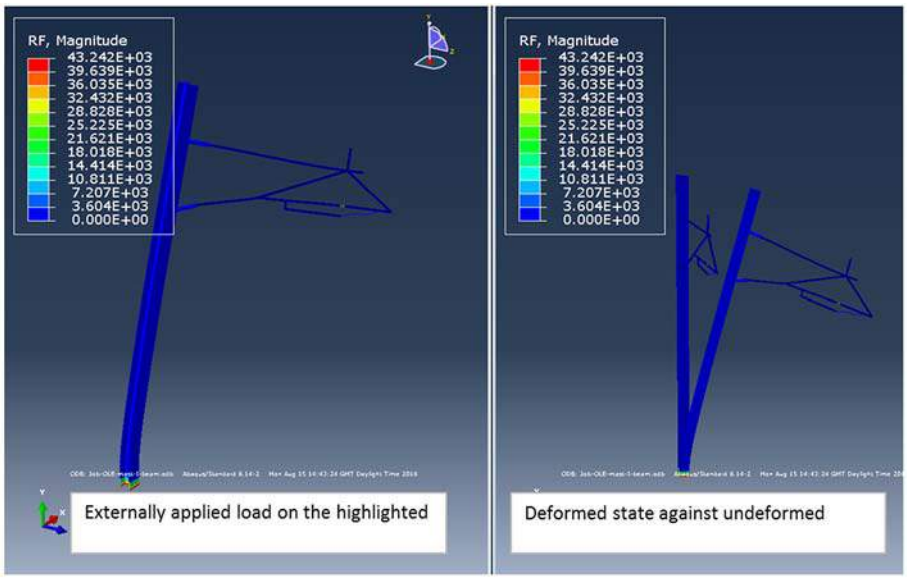

Figure 21 - (a) Along track reaction moment at OLE mast base (weak I beam section direction) and (b) Across track reaction moment at OLE mast base (strong I beam section direction).

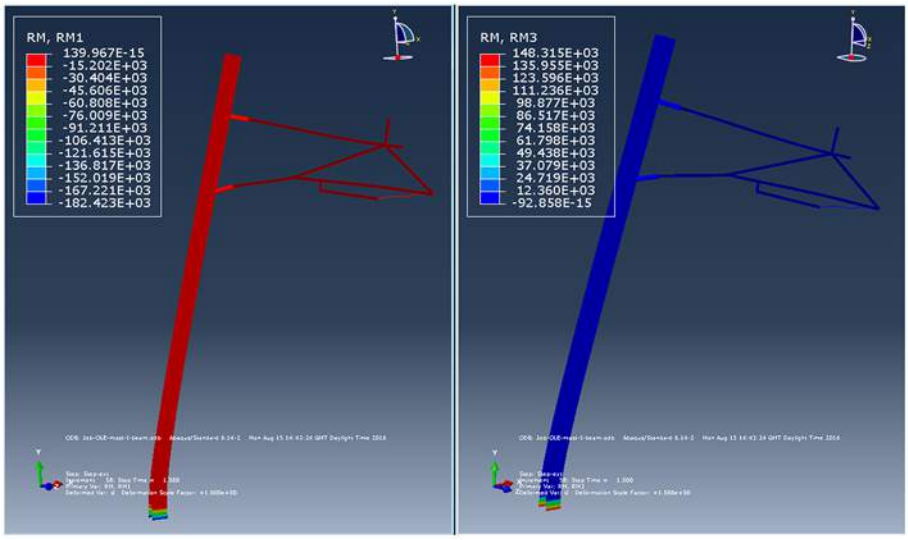

Figure 22 - (a) Equivalent plastic (permanent) strain magnitude at maximum deformation and (b) overall Mises stress criterion 3D contour rendering. The yield limit (355MPa) has been surpassed.

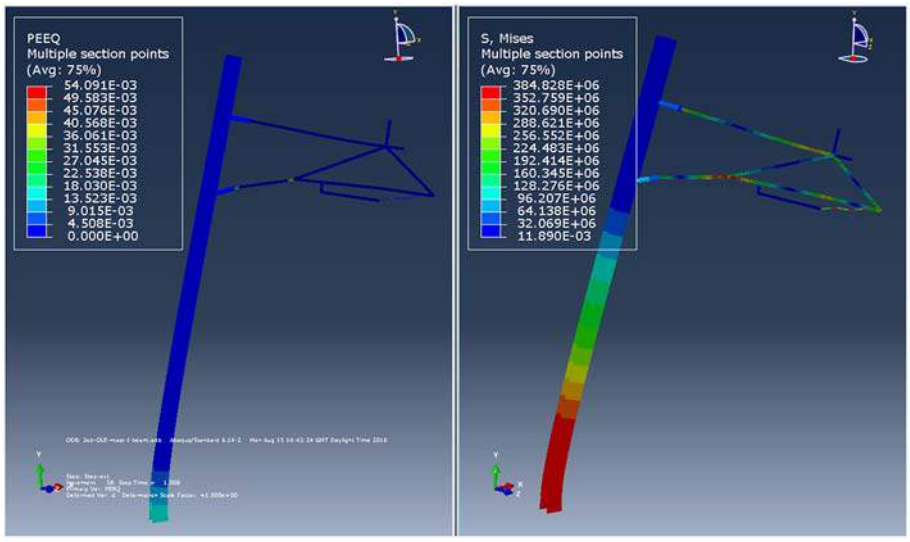

Figure 23 - Permanent mast deformation upon removal of external load application.

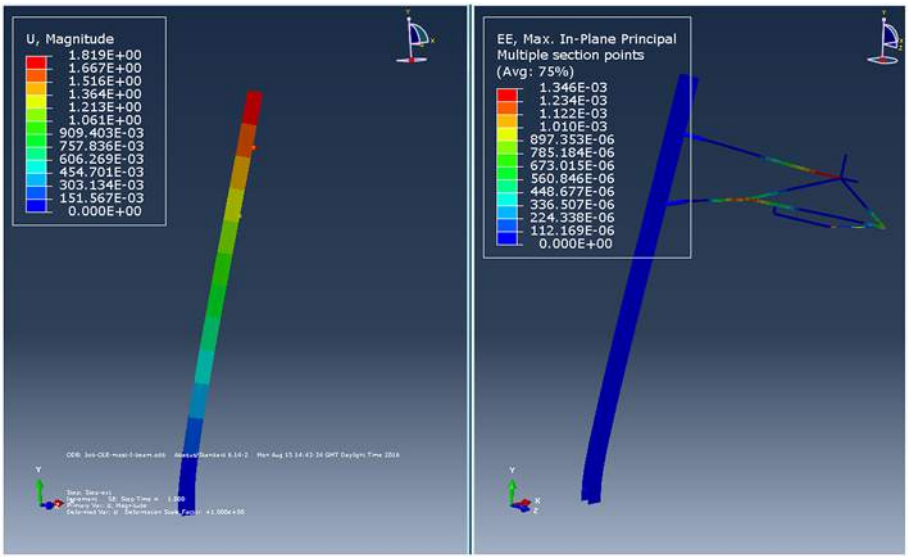

Note: On the right hand-side the image demonstrated that elastic strain is negligible and the remaining permanent deformation is 1.8m at the long end of the mast.

6.2 Three and four-foot pantograph deformation and stress distribution

Figure 24 - Overlap between deformed and un-deformed condition of 3-foot pantograph design.

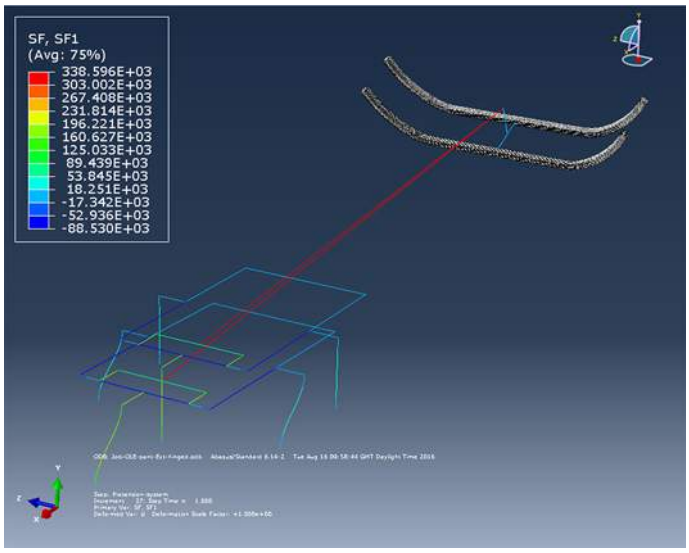

Note: Pantograph upper arm is locked to represent the pantograph / OLE cantilever engagement during a de-wirement.

Figure 25 - Von Mises stress criterion for 3-Foot (left) and 4-foot (right) pantograph.

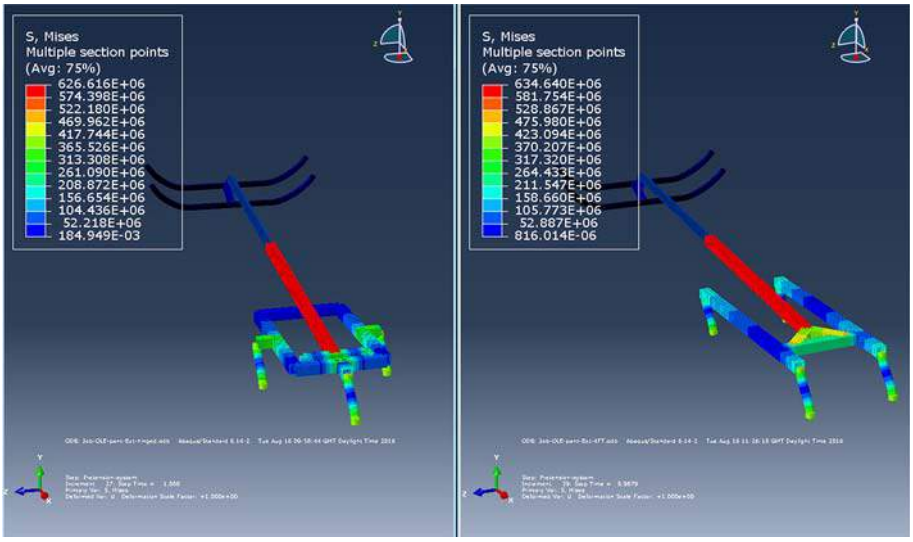

Note: At this stage the pantograph will apply a 352kN of force onto the STC (see Figure 28), the chain at pantograph elbow has failed (hence the pantographs are fully stretched) and the pantograph arms are fully released.

Figure 26 - Axial force distribution at the foot insulators for 3-foot (left) and 4-foot (right) of the pantograph.

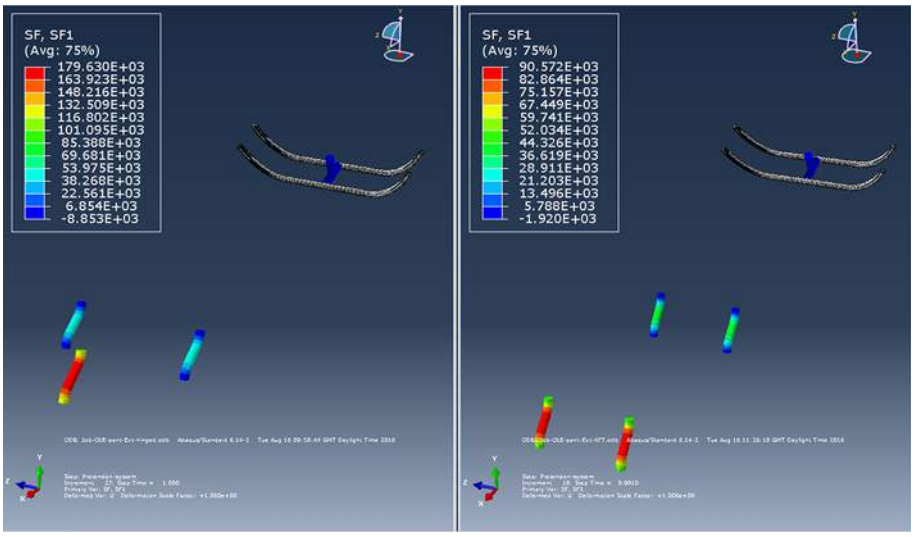

Figure 27 - Force distribution perpendicular to axial direction at the foot insulators for 3-Foot (left) and 4-foot (right) of the pantograph.

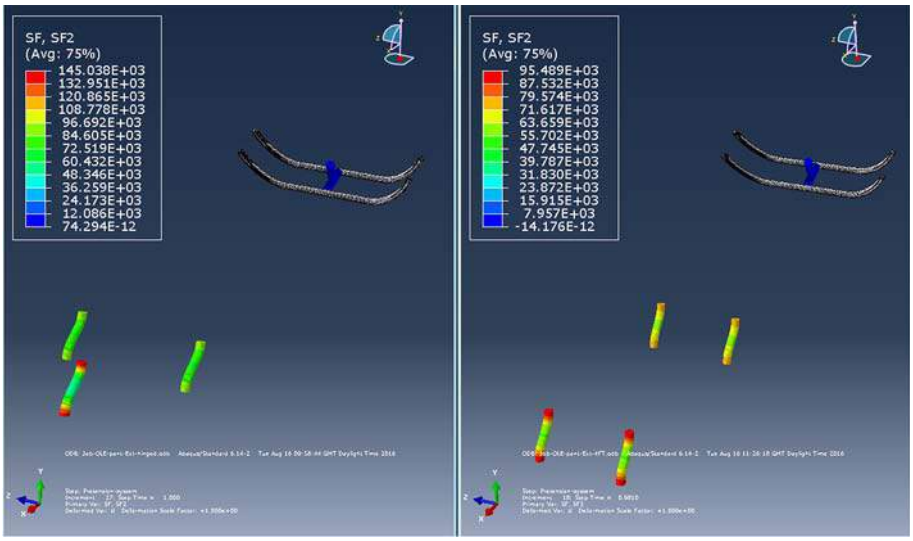

Figure 28 - Shear force distribution at the foot insulators for 3-foot (left) and 4-foot (right) of the pantograph.

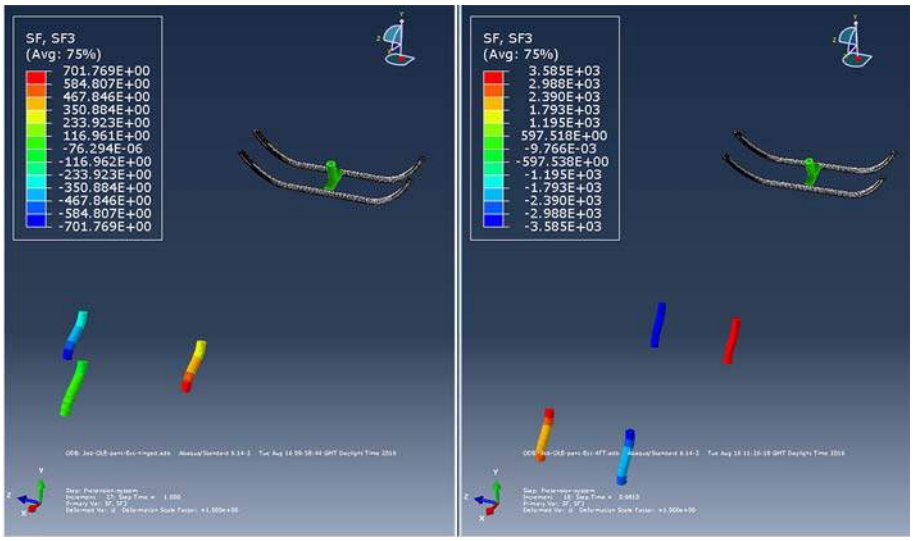

Figure 29 - Reaction force due to the engagement of the top pantograph arm to the OLE cantilever.

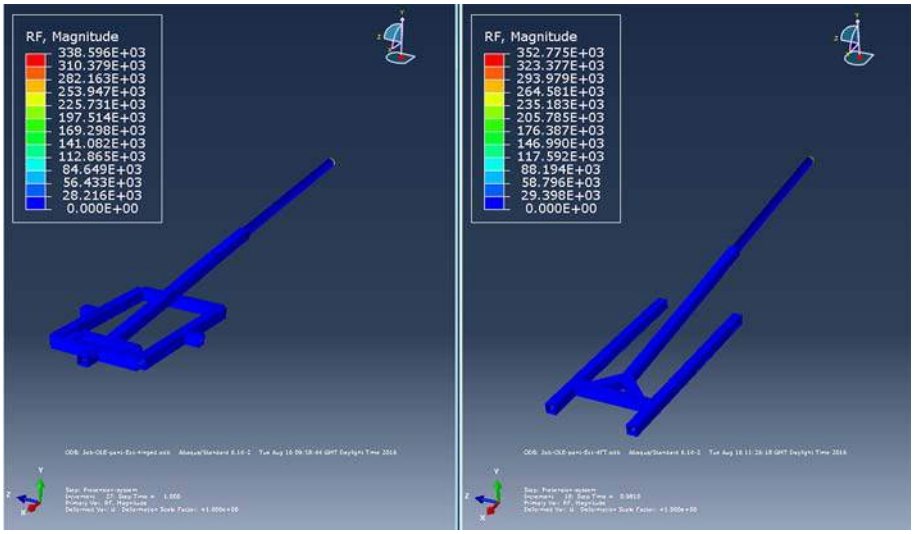

Figure 30 - Reaction force due to the engagement of the top pantograph arm to the OLE cantilever.

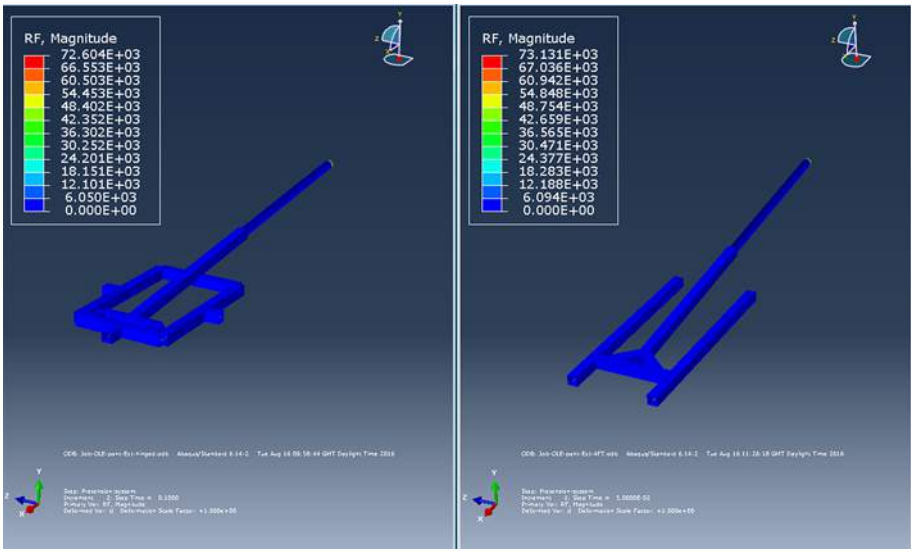

Note: At this force the OLE mast has been permanently deformed.

Figure 31 - Axial force distribution at the foot insulators for 3-foot (left) and 4-foot (right) of the pantograph.

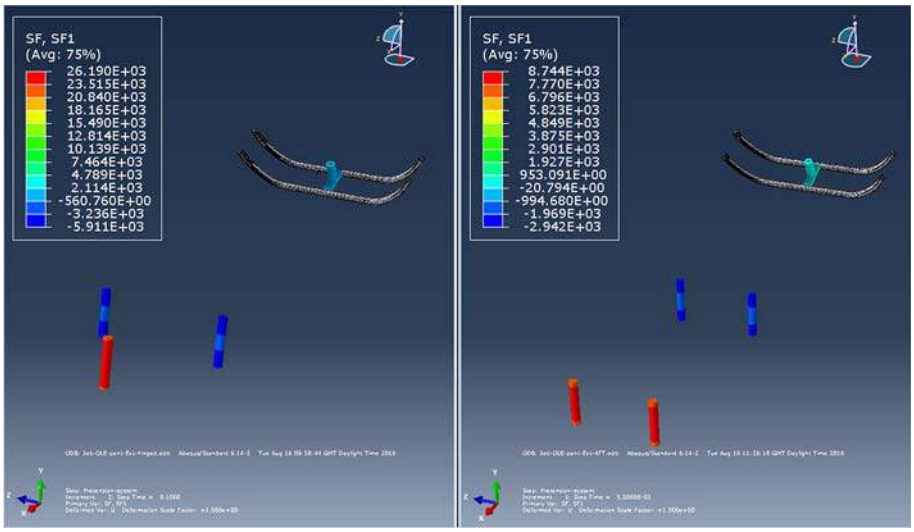

Figure 32 - Axial force distribution at the foot insulators for 3-foot (left) and 4-foot (right) of the pantograph.

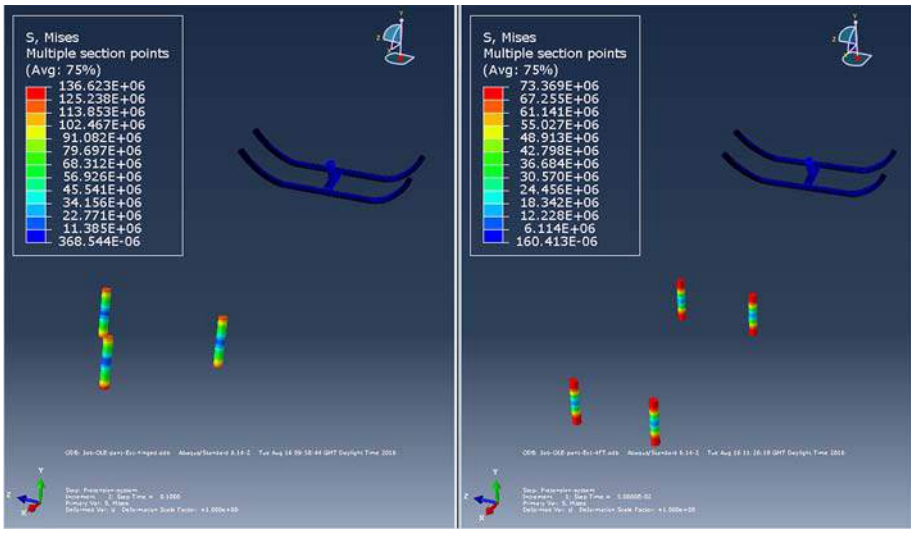

7 Discussion

7.1 Findings from previous report on the desktop review of incident reports

The review was hampered by the lack of detail in the incident reports after 2011, the Network Rail reporting could be improved by:

- The fitting of cameras to the roof as an evidence gathering tool during the investigation.
- Instigation of an incident investigation training course where engineers can develop best practices.

The above initiatives would allow future investigations to be more factual and meaningful and permit any resultant reports to be readily analysed.

7.2 Littleport incident review

It is evident that the pantograph did not fail as described in the RAIB report but there is insufficient documented evidence or photographs to come up with a more plausible scenario.

Any modifications to the pantograph or OLE cannot be designed to prevent such incidents as it has been incorrectly described in the RAIB report.

7.3 Understanding the forces and energy in the electrification system during a de-wirement

The results demonstrate the energy dissipation through the pantograph and OLE system during a de-wirement incident. It has been proven that the direction of travel of the pantograph plays a pivotal role into the resulting geometry of the 'unfolded' pantograph due to the inherent pantograph geometry and constrains.

When the pantograph moves in a knuckle leading position this results in the lower arm reaching maximum angular displacement, which will enable it to impact the OLE system with severe consequences.

When the pantograph moves, knuckle trailing the geometry will allow it to unfold. As a result, it is possible to amend the design to control the failure mode for the pantograph head connection to the top arm and a second design amendment at the knuckle, between upper and lower arms.

7.4 Ceramic insulators

Type testing demonstrated that the lowest cantilever load that will result in breakage of a single **ceramic pantograph foot insulator** was 18.4 kN.

The FE model showed that the maximum tensile stress will be 93MPa. Using this value as a threshold it has been found that the **ceramic cantilever insulator** will fail at 7.45kN of applied cantilever load.

7.5 Polymeric insulators

No testing to destruction data was available for the polymeric insulators. The material properties were calibrated using experimental test results along with the ultimate strength for bending which is stated by the manufacturer to be 900MPa. This figure has been the threshold used for the purposes of analysing the individual component capacity. However, it has to be noted, that based on experimental observations, at 900MPa there will be an excessive amount of deformation. Hence, the point where excessive plastic deformation is observed has been ultimately used as an indication for insulator failure, However, this does not guaranty separation or load removal from infrastructure

For the **polymeric pantograph foot insulator**, the same 18.4kN cantilever load was applied giving 115MPa Von Mises stress. At the same time the insulator end fittings will sustain 215MPa. A common aluminium alloy will typically have a yield limit of 276MPa and ultimate strength of 310MPa. Therefore, it is anticipated that the insulator will fail primarily due to detaching from the base at a much higher load. It has to be noted that the pantograph foot insulator (Figure 13) has a very long crimped interface between the aluminium holder and the polymer insert which significantly strengthens the component.

For the **polymeric cantilever insulator** material data were calibrated to the values provided on the NR drawing. A 5.6kN load was applied to represent the 3kNm ultimate bending moment capacity. At this load 214MPa Von Mises

stress was sustained by the polymeric part and 217MPa by the aluminium end caps. The insulator is expected to withstand higher load before the insulator ends separate from the polymeric core.

7.6 OLE structure

The **OLE STC Series Mark 3B_** with a 254x254x73 UKC steel section was simulated to retrieve the amount of force required to cause plastic deformation to the OLE mast during a de-wirement incident. It has been found that the mast will be permanently deformed at when the load exceeds 43kN as applied by the pantograph.

7.7 Three and four foot pantographs

A global analysis was deployed for the **3-foot** and **4-foot** pantograph models **with polymeric insulators**. It has been demonstrated that at an applied load of 352kN on the pantograph strip will cause the lower 80 x 80 x 8mm box section of the pantograph to reach 626MPa for the case of a 3-foot insulator and 634 MPa for the 4 foot insulator. At this stage the polymeric insulator will still be able to sustain the load due to their 900MPa ultimate capacity limit. There are no records of loads being applied to the pantograph in case of a de-wirement incident. It is also unlikely that the OLE system will be able to apply this load to the pantograph. It is very important to state that for the purposes of the project static problem formulation has been used. As a result the forces cannot realistically represent the dynamic impact process that will occur in case of a de-wired moving pantograph being captured by the OLE cantilever structure.

Static loading was also applied on **4-foot pantograph with ceramic insulators**. The analysis of stress distribution to the system suggests that the ceramic insulator will reach their cantilever loading capacity with the application of 70kN of force to the pantograph. However, the ceramic foot insulator behaviour under dynamic impact loading is expected to be significantly different. Therefore, it is suggested that this number is only used for comparison with the equivalent polymeric counterparts and not a scientifically sustained numerical solution.

8 Conclusions

The following has been calculated:

- Ceramic pantograph foot insulator = 18.4kN maximum fracture load in shear
- Ceramic cantilever insulator = 7.45kN maximum fracture load in shear
- Polymeric pantograph foot insulator = 900 MPa maximum capacity of polymeric core in shear
- Polymeric cantilever insulator = 217MPa minimum load capacity in shear
- Permanent deformation of OLE structure = 43kN in along-track force applied on single-track cantilever (STC)
- Three and four-foot pantograph with polymeric insulators = 352kN due to tensile failure of the top pantograph arm.
- Four-foot pantograph with ceramic insulators = 70kN due to shear failure of pantograph foot insulators

9 Recommendations

Based on the findings of this report the following recommendations should be considered:

- To allow realistic loads and energy dissipation amongst the system components it is proposed to pursue a dynamic finite element (FE) simulation of impact between passing pantograph (both directions) against an OLE mast.
- The design implementation of the proposed fail safe components for pantographs and OLE cantilever requires a rigorous FE assessment to specify mechanical strength and comparative component resistance to failure in the case of a de-wirement incident. Mechanical testing of the proposed concept fail-safe device components is a minimum requirement to validate and substantiate the FE investigation.

Section 2: Controlling the failure modes of the pantograph and OLE structure during a de-wirement

10 Controlling the failure modes of the OLE structure

The OLE STC mast will sustain severe plastic deformation due to impact with the pantograph and due to the inherent strength of the polymeric insulators that can hold up to 1400MPa in tension, which exceeds by far the capacity of steel components within the STC assembly (theoretically the 45mm Ø cantilever insulator will sustain minimum 2000kN before it breaks).

Figure 33 - Polymeric insulator drawing with additional schematic representation of the proposed fail-safe release mechanism in case of impact tensile load application.

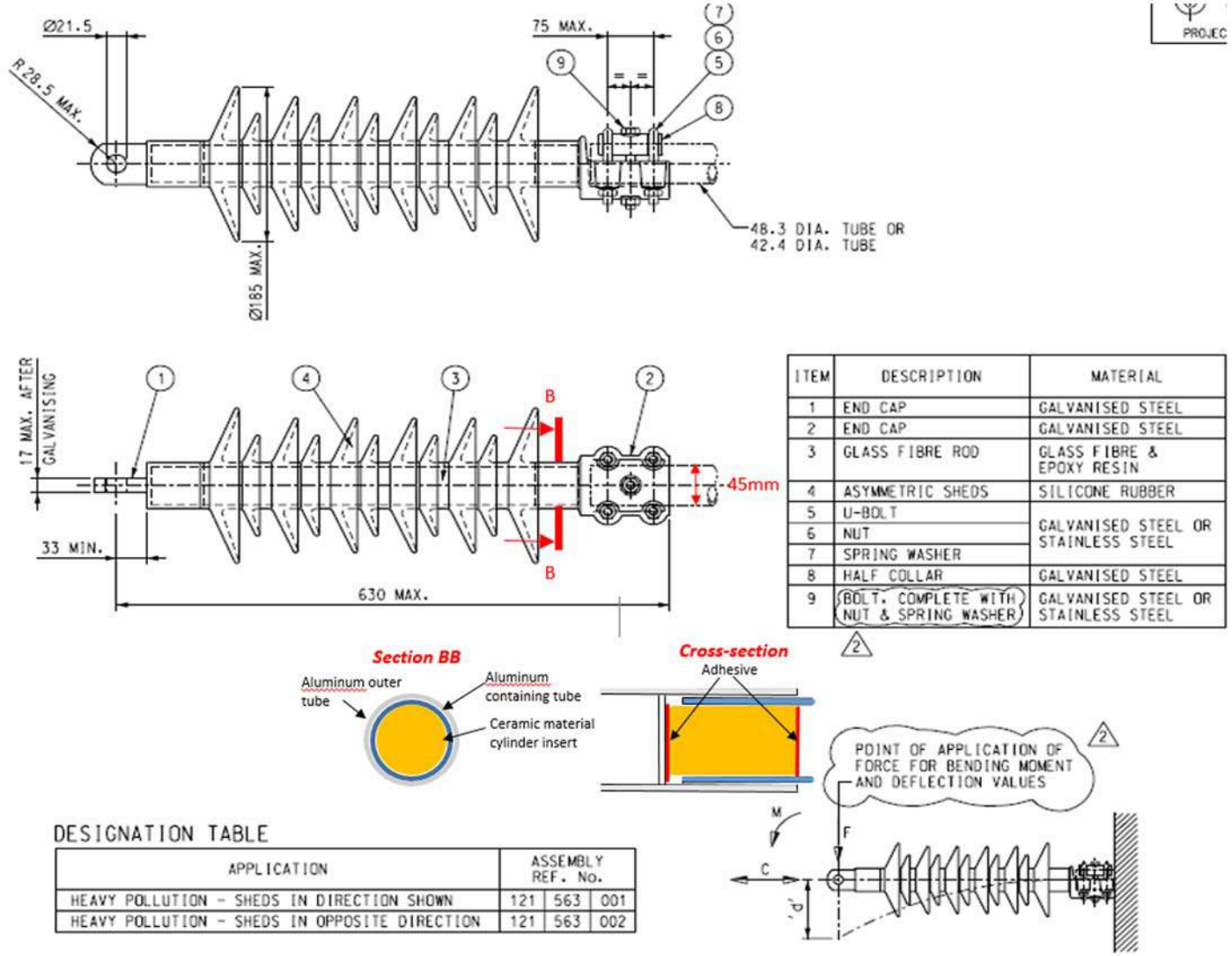

ITEM	DESCRIPTION	MATERIAL
1	END CAP	GALVANISED STEEL
2	END CAP	GALVANISED STEEL
3	GLASS FIBRE ROD	GLASS FIBRE & EPOXY RESIN
4	ASYMMETRIC SHEDS	SILICONE RUBBER
5	U-BOLT	GALVANISED STEEL OR STAINLESS STEEL
6	NUT	
7	SPRING WASHER	
8	HALF COLLAR	GALVANISED STEEL
9	BOLT, COMPLETE WITH NUT & SPRING WASHER	GALVANISED STEEL OR STAINLESS STEEL

APPLICATION	ASSEMBLY REF. No.		
HEAVY POLLUTION - SHEDS IN DIRECTION SHOWN	121	563	001
HEAVY POLLUTION - SHEDS IN OPPOSITE DIRECTION	121	563	002

The variety across OLE design ranges (Series 1, 2, Mark 3B, etc.) increases the implications for finding a global fail-safe system design. The most common part appearing in most of the OLE structure assembly types (STC, TTC, portals) is the insulator itself which in most cases generally separates electrically and mechanically the 'live' CW from the rest of the structure. Usually the insulator end which attaches to the structure allows for a hinged connection to avoid transmitting torsion to the slender OLE mast and bending to the insulator. On the other end of the insulator a U-bolt connection is usually designed to attach the insulator directly to the registration arm or other stove pipe components (see Figure 33).

A proposed schematic in Figure 33 provides a feasible solution for a fail-safe component design that will cause the insulator end (closer to the train) to break in tension in case of a de-wirement. The proposed design aims to:

- Separate the OLE cantilever from the insulator excluding the insulator and associated weight from being released.
- Provide guidance to the ceramic inclusion to ensure that bending loads are not transmitted to the ceramic insert (slide-in assembly).
- Allow very precise determination of the failure load required at different impact speeds.

This is a system solution that can be further investigated in terms of manufacturing and mechanical feasibility. Appropriate material should be determined and tested (statically and impact) for the ceramic insert and appropriate adhesive should be used to safely bond the interface.

11 Controlling the failure modes of the pantograph

Presently the principal method of controlling failure as a result of interface issues is achieved by integration of an auto-drop detection system. However, this only guarantees that the driver is aware of an incident and initiates the pantograph dropping. It detects an incident but does not prevent the loadings incurred.

Methods of limiting forces generated between the vehicle and the infrastructure proposed are:

11.1 Head separation

The pantograph head is encouraged to separate hence reducing overloading forces. This can be achieved by reducing the strength of pantograph head pivot bracket mounted to the top of the head suspension (applies to HSP type units only) as in Figure 34.

The normal force distribution within the pan head support is within the lower quadrant of contact. The principal direction of force is vertical, with a horizontal component generated by aerodynamic drag and friction at the interface. There is no upward component of force on the head excepting minor aerodynamic influences under abnormal conditions, or during transit with the pantograph housed, the reaction from the head rests. Given these forces are low, the top of the head retention can be modified to a significantly reduced section and limit the forces generated at separation.

Figure 34 - Reducing strength of pantograph head pivot bracket

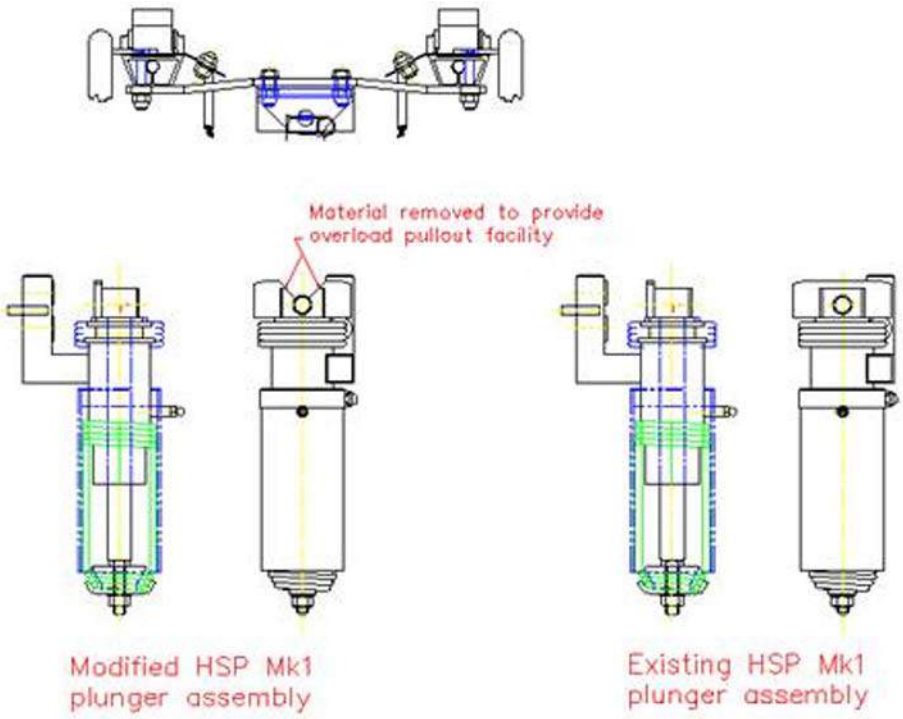

11.2 Cross tube separation

The other key item which may engage with the infrastructure is the cross tube and suspension assembly. Again the loading is predominantly the lower quadrant of the bearing housings although in this case the bearing housing rotates through 45-50 degrees as the pantograph rises throughout the operating range.

However, a similar approach can be applied to this arrangement, placing the point of weakness on the upper rearward portion of the bearing housing. As this is a fabricated assembly it is proposed that the weakening be applied by forming a large hole with minimal perimeter wall thickness as in Figure 33.

Figure 35 - Reducing the strength of cross tube bearings

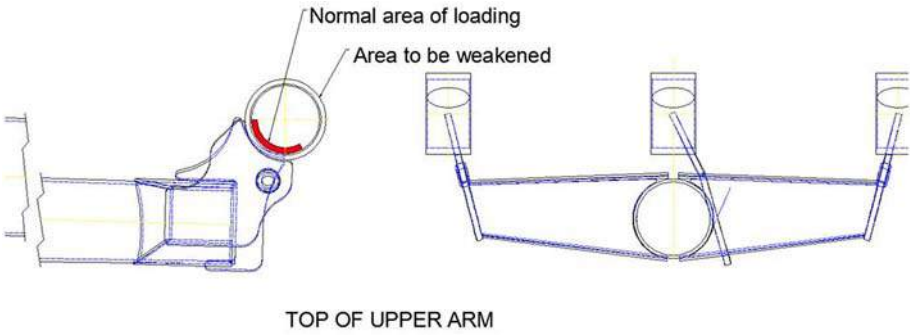

11.3 Upper arm separation (elbow failure mode)

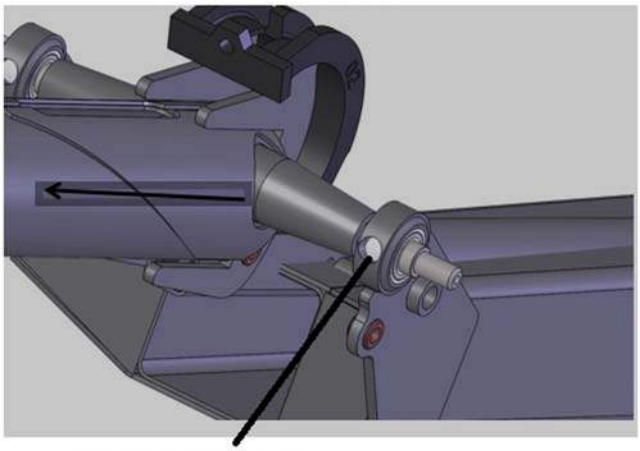

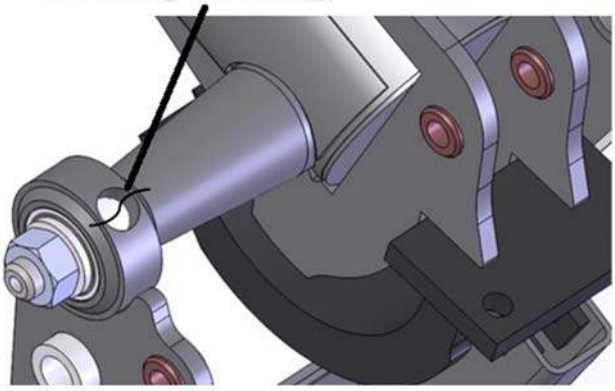

In the event that the above failure modes are insufficient to totally separate the pantograph from the infrastructure, it is usually the case that the elbow chains fail as a result of the excessive turning moment applied to the upper arm. This releases the upper arm to rotate relative to the rest of the pantograph structure, but does not separate the arm from the vehicle.

A final point of frangibility could be provided at the elbow assembly by applying a similar philosophy (as in Section 2.2) to the elbow bearing housings in the lower arm fabrication.

The provision of a radial hole in the stainless steel bearing housing at a location opposite to that which sees any loading in service gives a preferential point of separation. The retained wall thickness at the side of the hole would be minimized to reduce the load and hoop stress required to fracture, although this would still be significant given the bending strength of the housing material.

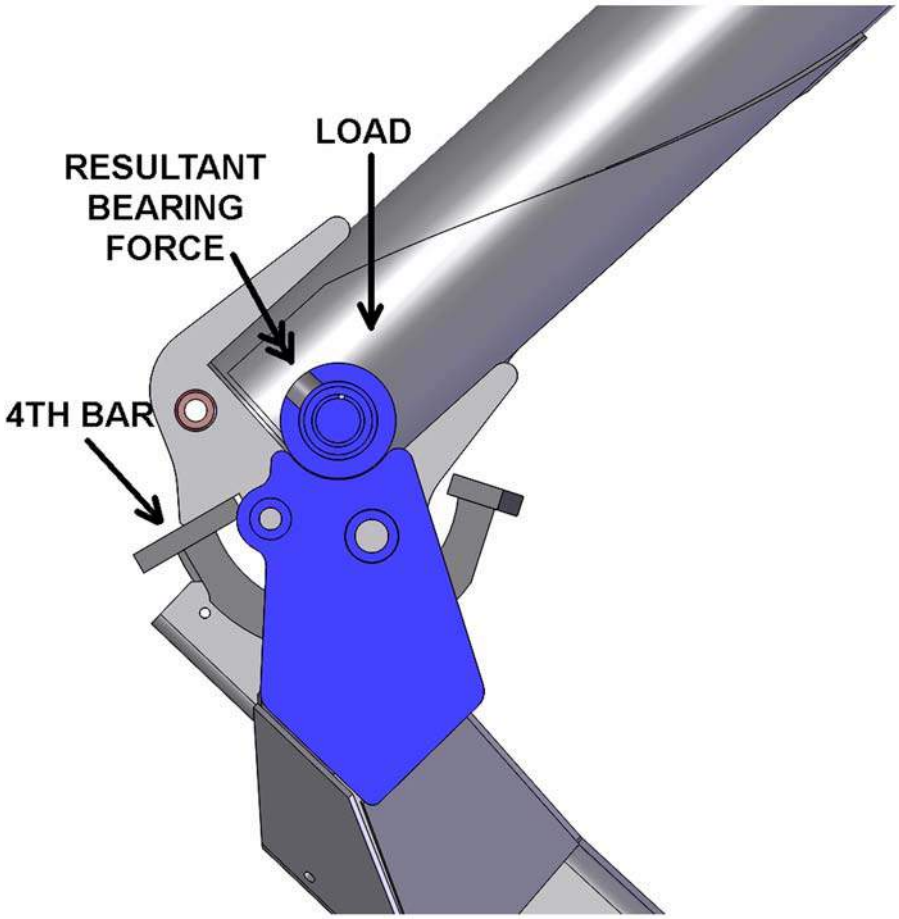
LOAD
RESULTANT
BEARING
FORCE
4TH BAR

12 Recommendations

The following recommendations should be considered:

- Precise information for individual material deformation parameters via mechanical testing will allow the optimisation of the fail-safe design implementation into pantograph and OLE system. Experimental investigation on proposed fail safe system components at material level.
- Experimental dynamic assessment on proposed fail-safe system components full scale assembly in a controlled environment.
- Once the final design and prototype fail safe devices are installed these should be tested individually to ensure that they behave as per FE mechanical simulation.

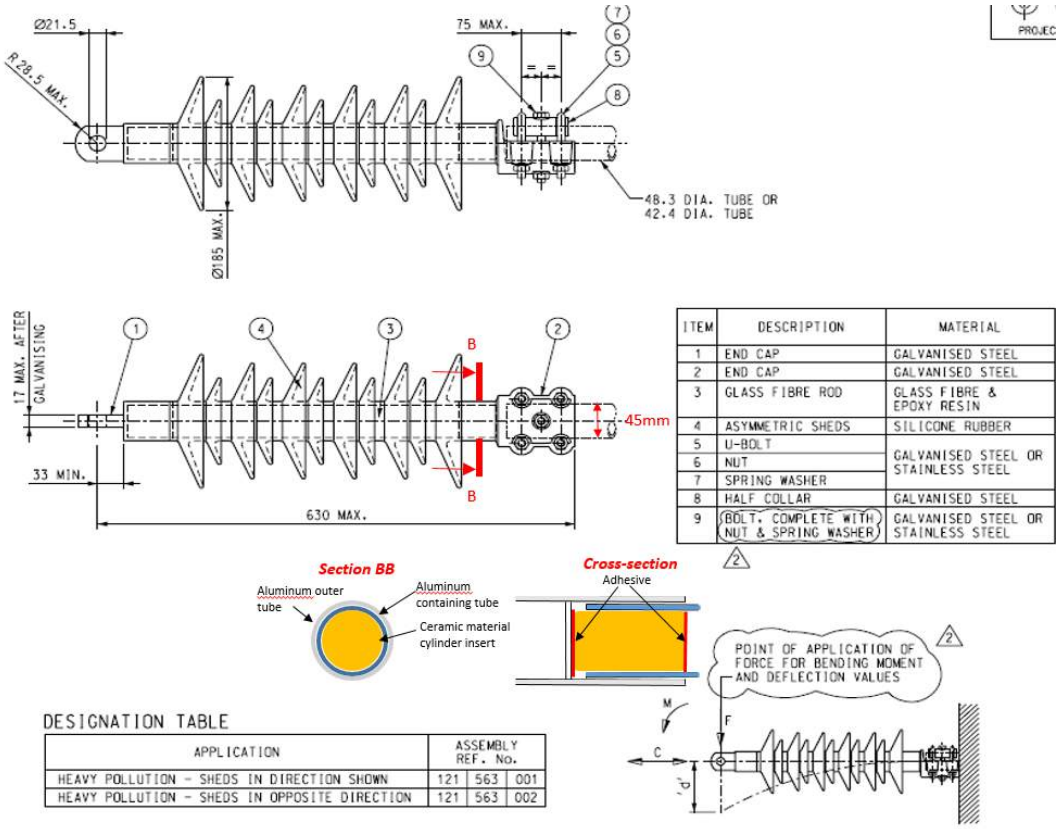

ITEM	DESCRIPTION	MATERIAL
1	END CAP	GALVANISED STEEL
2	END CAP	GALVANISED STEEL
3	GLASS FIBRE ROD	GLASS FIBRE & EPOXY RESIN
4	ASYMMETRIC SHEDS	SILICONE RUBBER
5	U-BOLT	GALVANISED STEEL OR STAINLESS STEEL
6	NUT	
7	SPRING WASHER	
8	HALF COLLAR	GALVANISED STEEL
9	BOLT, COMPLETE WITH NUT & SPRING WASHER	GALVANISED STEEL OR STAINLESS STEEL

DESIGNATION TABLE

APPLICATION	ASSEMBLY REF. No.		
HEAVY POLLUTION - SHEDS IN DIRECTION SHOWN	121	563	001
HEAVY POLLUTION - SHEDS IN OPPOSITE DIRECTION	121	563	002

13 Input drawings

Figure 36 - Ceramic 14'' Pantograph Foot Insulator

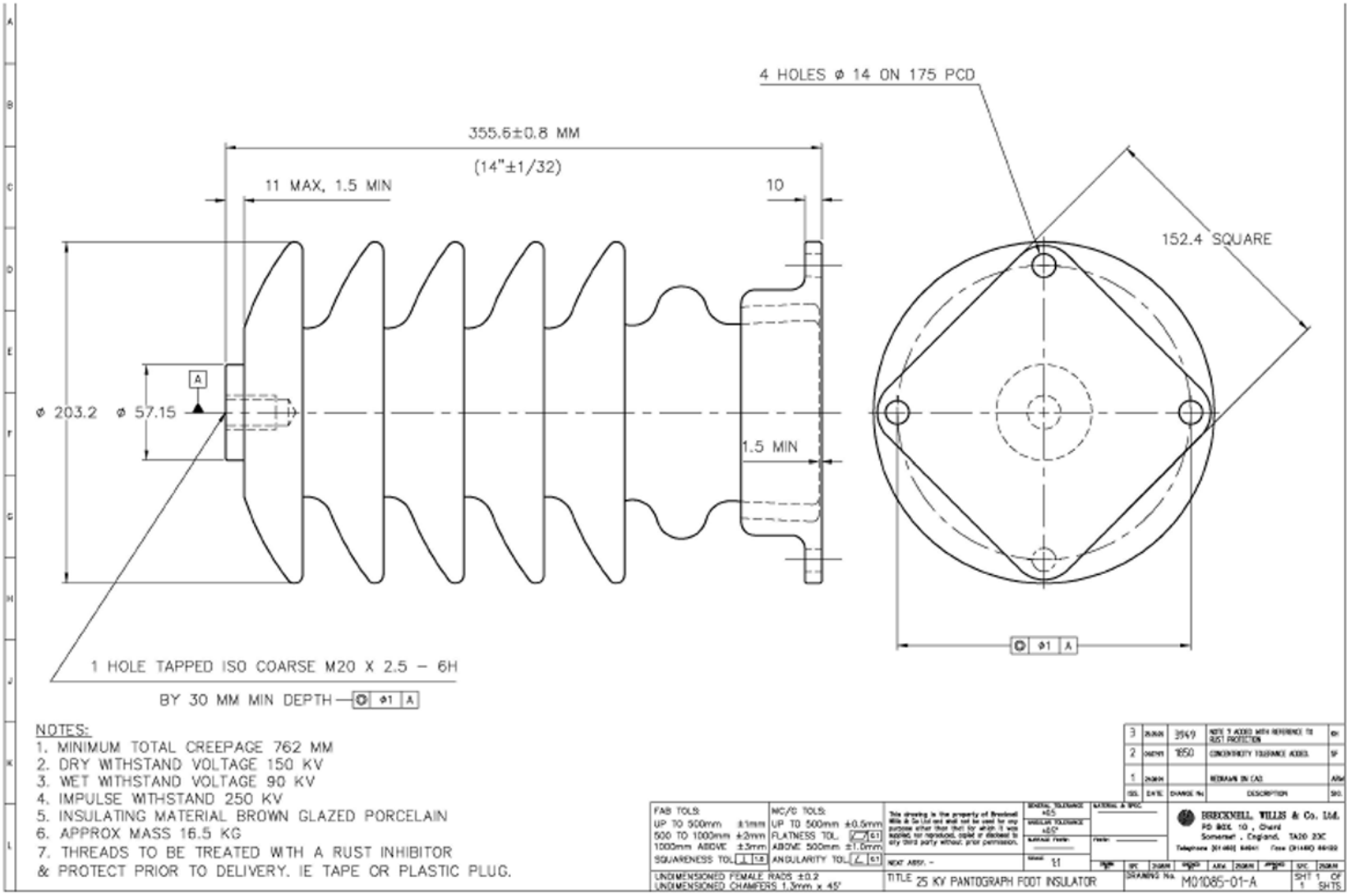

Figure 37 - Polymeric 14'' Pantograph Foot insulator

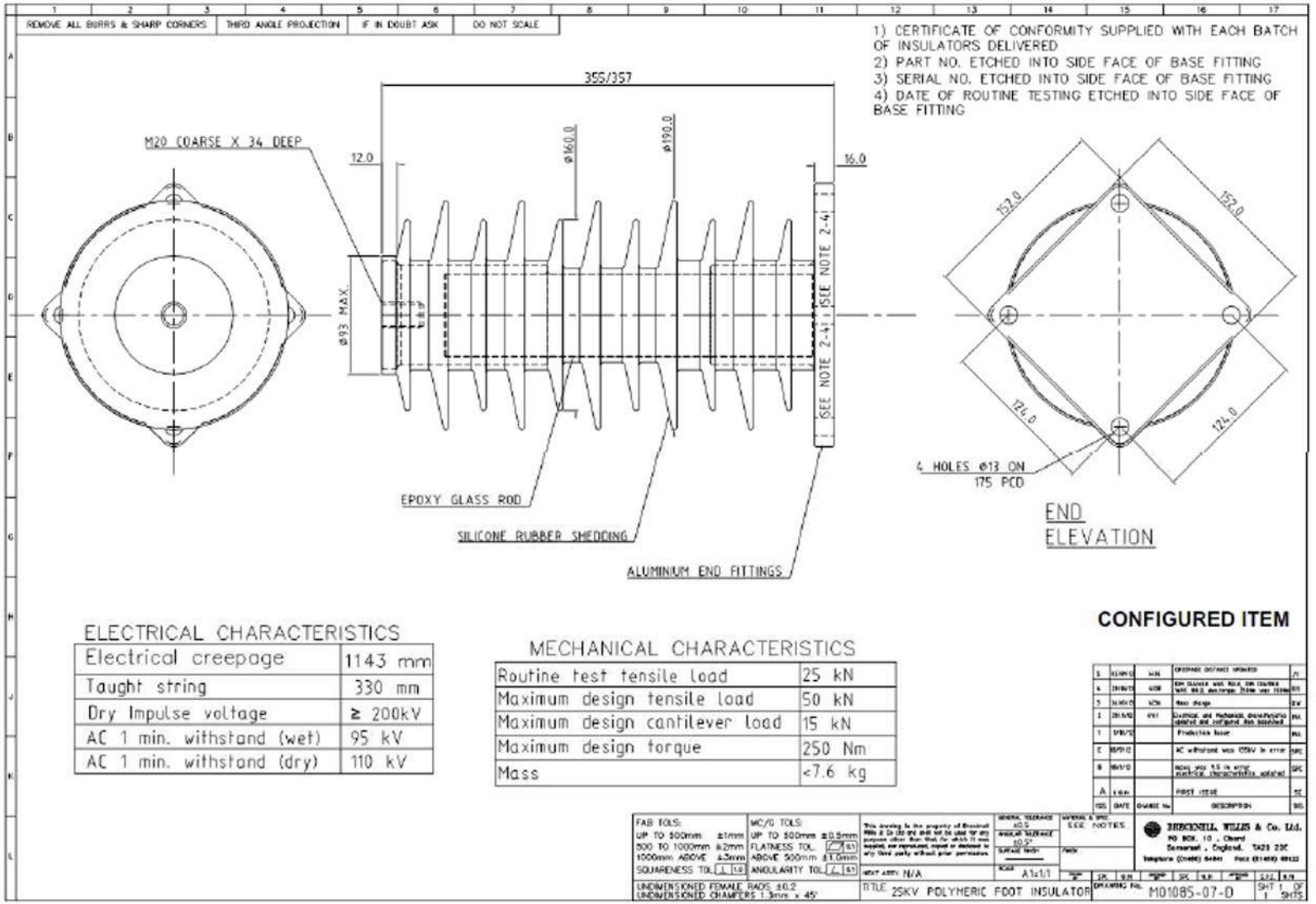

Figure 38 - Ceramic cantilever insulator

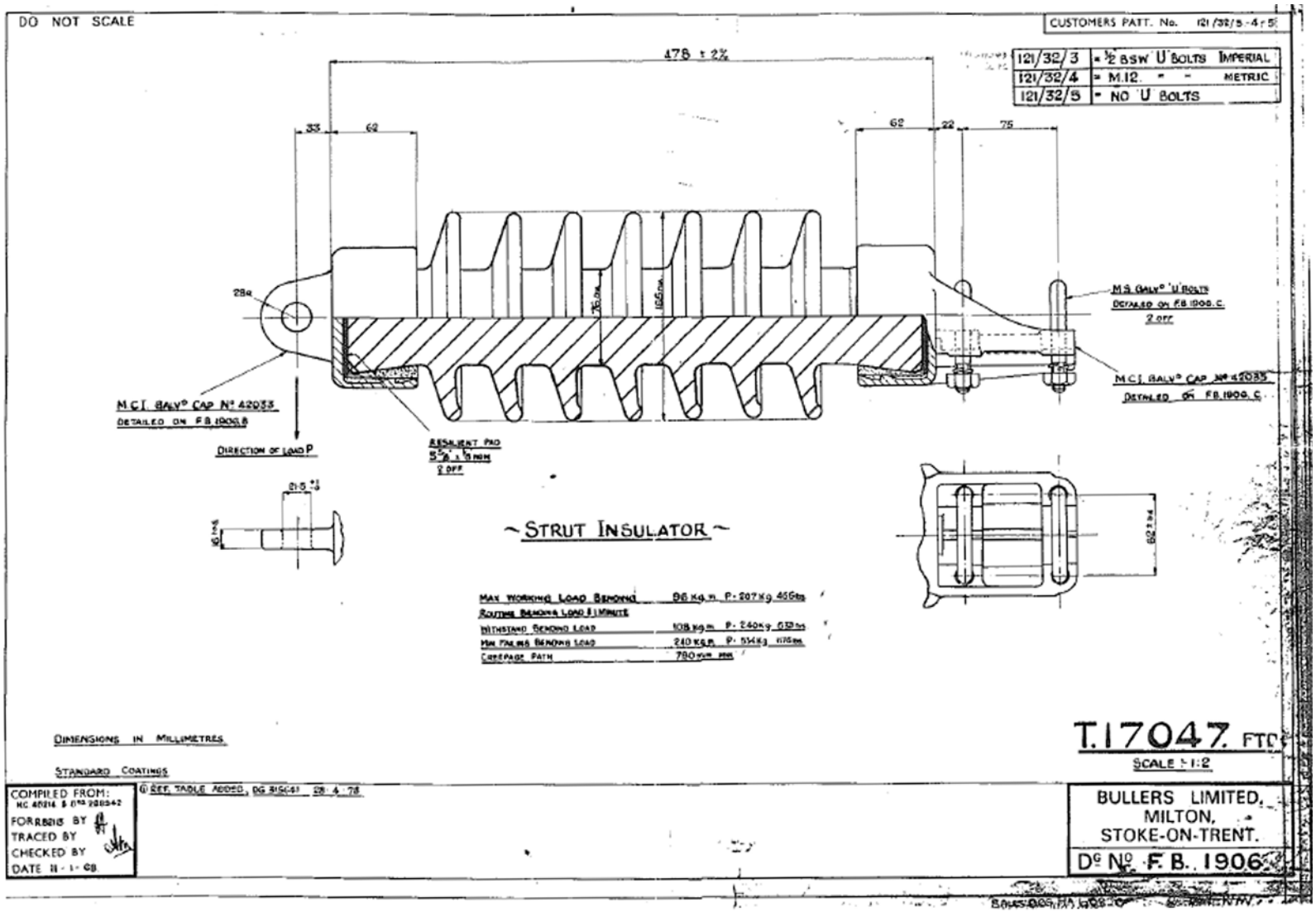

Figure 39 - Polymeric cantilever insulator

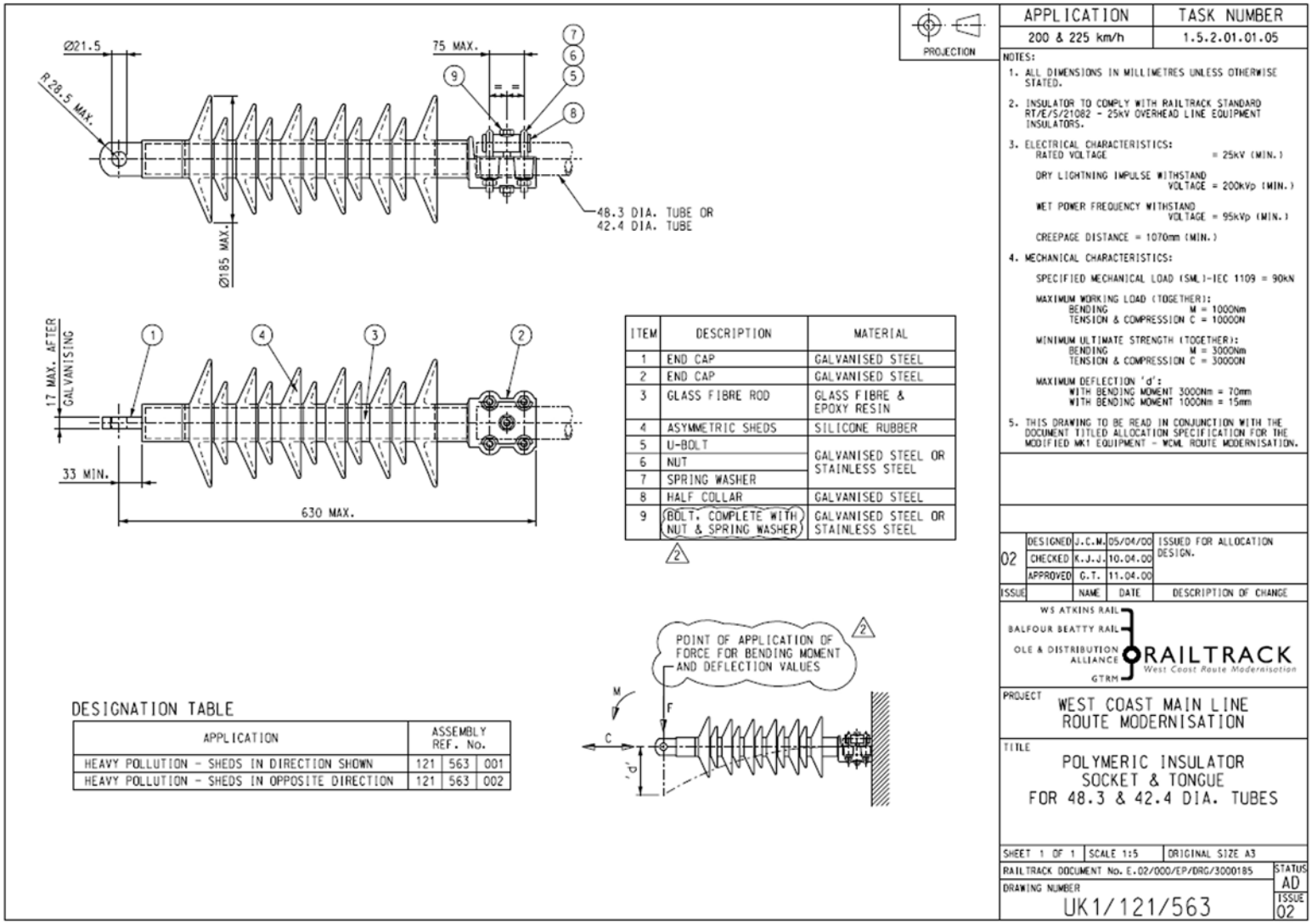

Figure 40 - 3-Foot Thameslink Pantograph GA – M00042-54-L

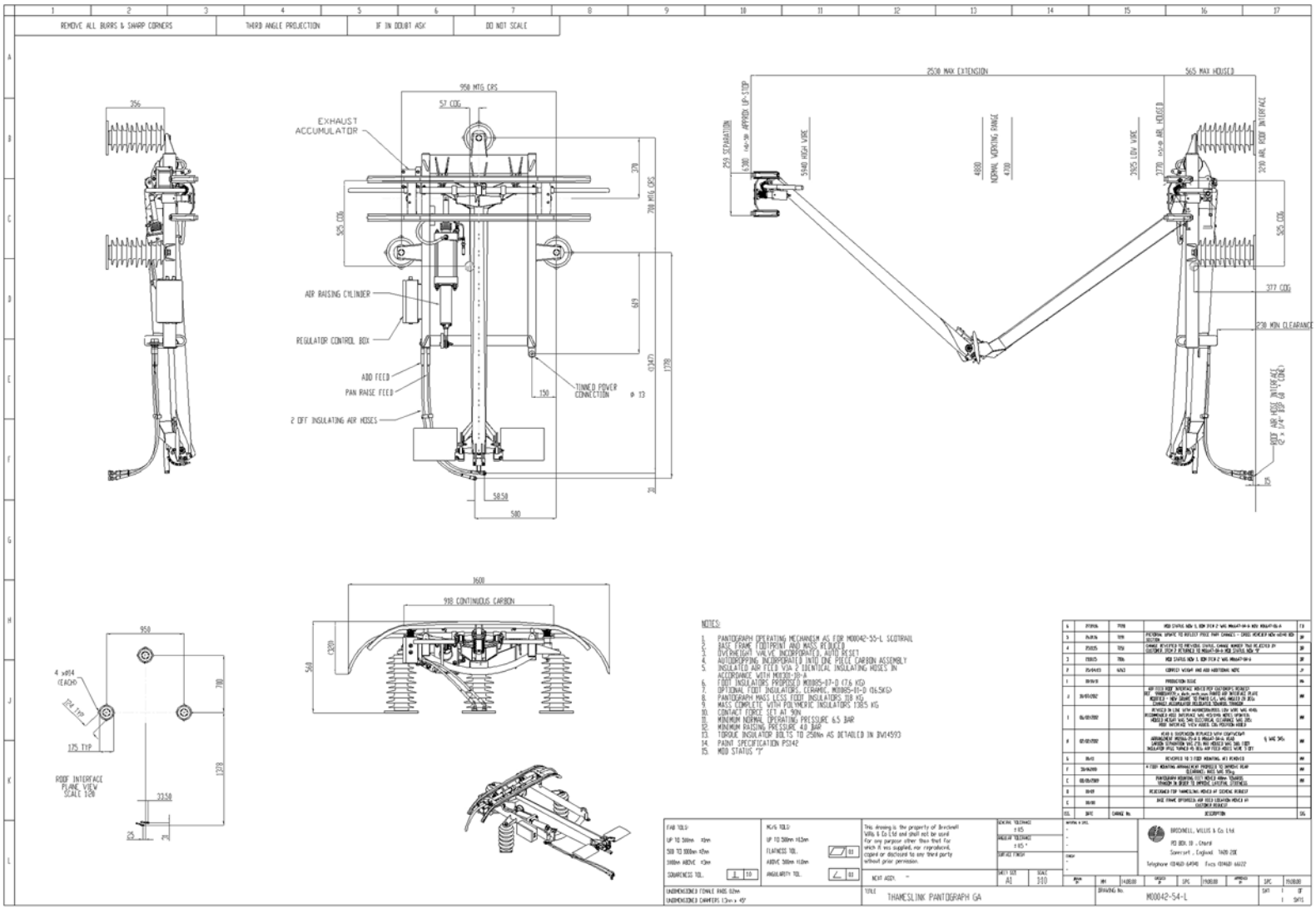

Figure 41 - 4-Foot GA CL91 Pantograph – M00042-10-L

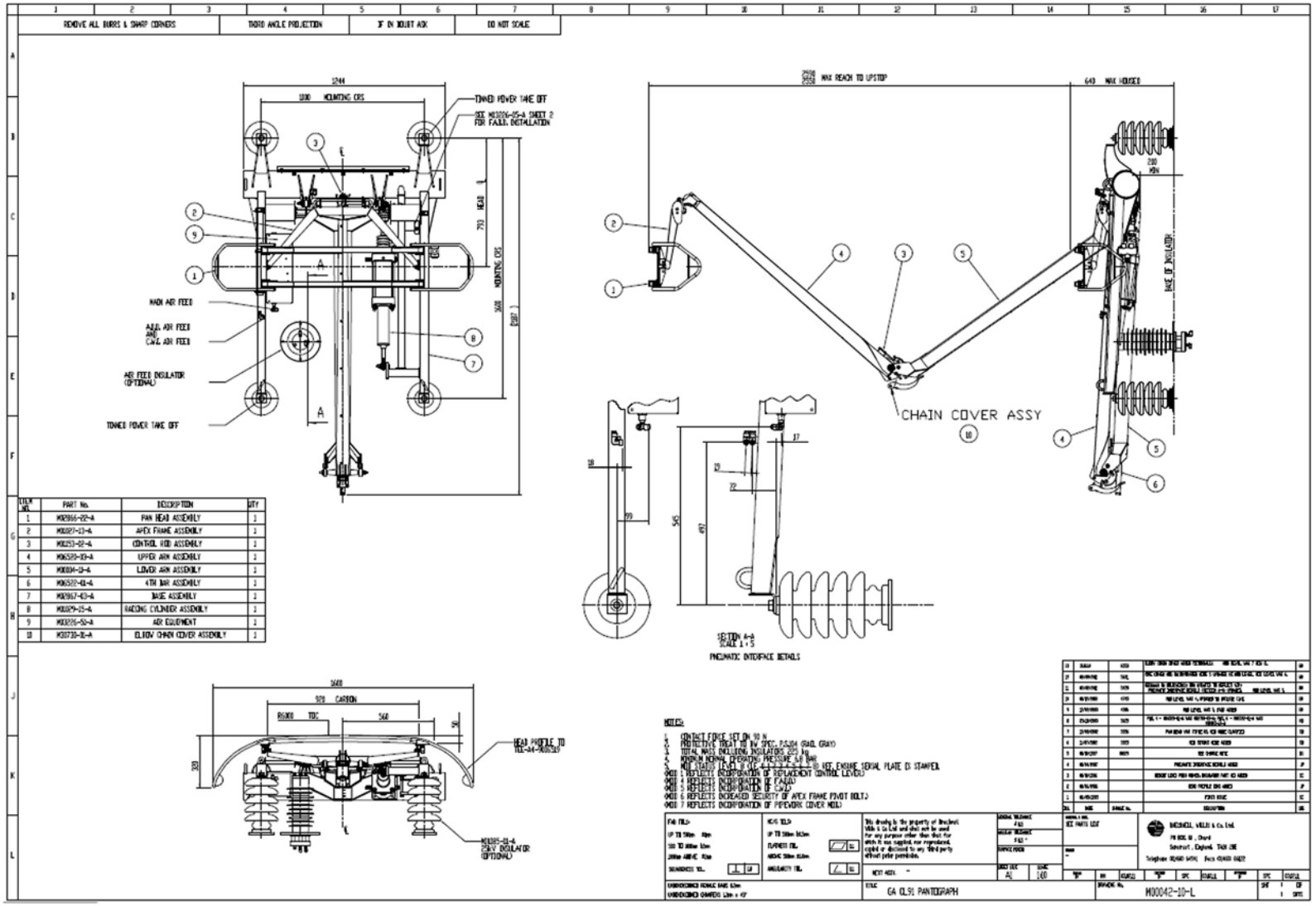

ITEM NO.	PART No.	DESCRIPTION	QTY
1	M00966-02-A	FAN HEAD ASSEMBLY	1
2	M00827-03-A	APEX FRAME ASSEMBLY	1
3	M00253-02-A	CONTROL ROD ASSEMBLY	1
4	M00520-03-A	UPPER ARM ASSEMBLY	1
5	M00804-03-A	LOWER ARM ASSEMBLY	1
6	M00522-03-A	4TH BAR ASSEMBLY	1
7	M00967-03-A	BASE ASSEMBLY	1
8	M00829-05-A	RAISING CYLINDER ASSEMBLY	1
9	M00826-02-A	AIR EQUIPMENT	1
10	M00730-10-A	ELBOW CHAIN COVER ASSEMBLY	1

Figure 42 - Mark 3B STC OLE Cantilever – 254x254x73 OLE mast installation

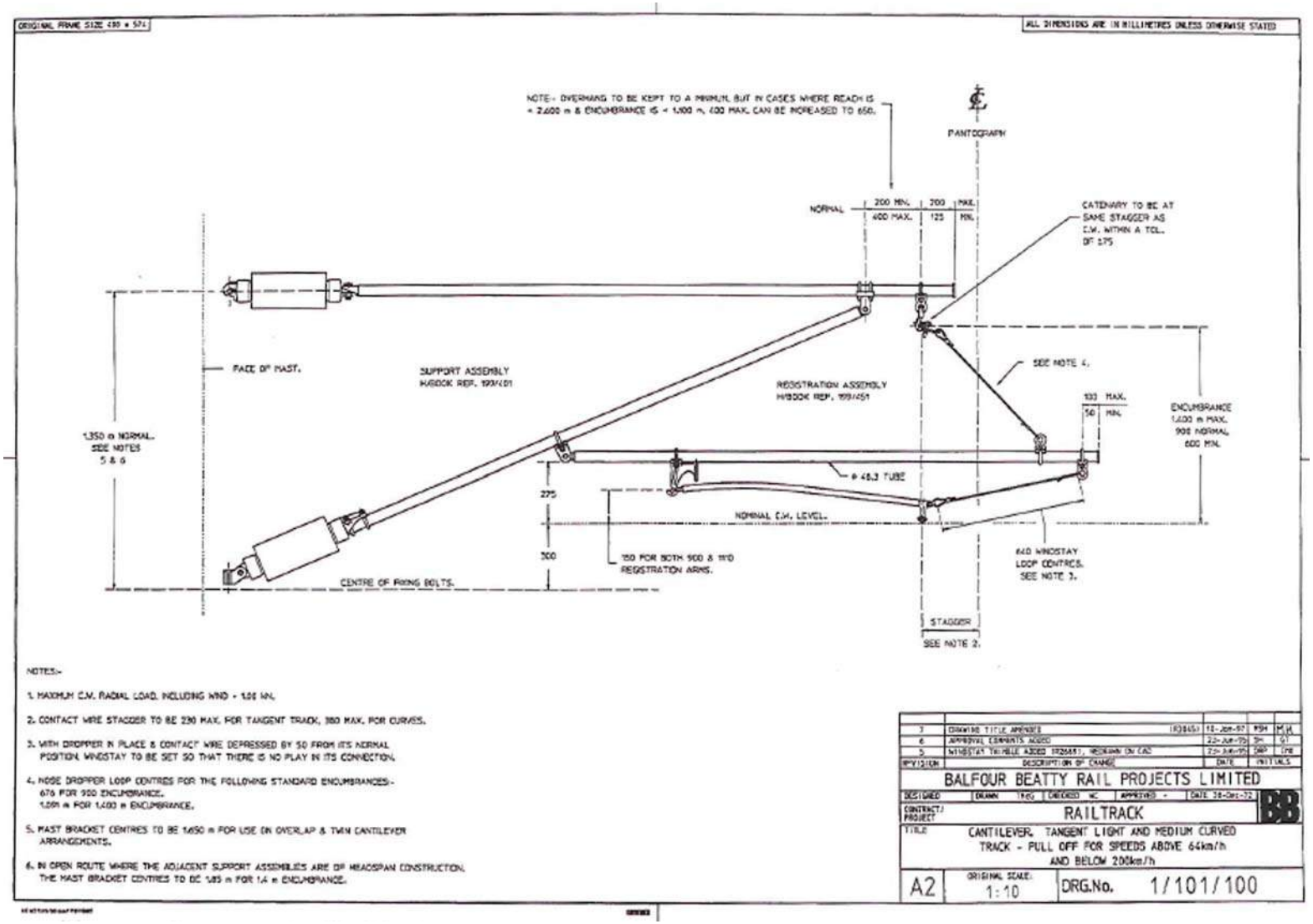

RSSB
Floor 4, The Helicon
1 South Place
London
EC2M 2RB

enquirydesk@rssb.co.uk

http://www.rssb.co.uk